

---

# AN MCNP6 PRIMER

---

by

**J. Kenneth Shultis**  
(jks@ksu.edu)

and

**Amir A. Bahadori**  
(bahadori@ksu.edu)

Alan Levin Department of Mechanical and Nuclear Engineering  
Kansas State University  
Manhattan, KS 66506

(c) Copyright 2004–2024  
All Rights Reserved

## Notice

This primer is a revision of an earlier one for MCNP5 and is intended for use by students in our course NE690, Radiation Protection and Shielding, who are introduced to MCNP for the first time. Thus, this primer is mainly oriented towards fixed-source, steady-state applications involving neutrons and photons. The authors acknowledge that this primer presents only a tiny fraction of the vast capabilities of MCNP6.

Although this primer is the property of the authors, we give permission for others to freely copy and distribute it provided no changes are made to it. We would appreciate receiving error corrections or suggestions for improvements so that future versions of this primer are enhanced.

A sporadically updated errata for this primer, as well as the primer itself, can be found on the world wide web at <http://www.mne.ksu.edu/~jks/books.htm>. Revised versions, when created, will also be made available on this web site.

## Contents

<b>1</b>	<b>Structure of the MCNP Input File</b>	<b>2</b>
1.1	Annotating the Input File . . . . .	2
1.2	Units Used by MCNP . . . . .	3
<b>2</b>	<b>Geometry Specifications</b>	<b>3</b>
2.1	Cells – Block 1 . . . . .	5
2.2	Macrobodyes . . . . .	6
2.2.1	Unstructured Meshes . . . . .	8
<b>3</b>	<b>Data Specifications – Block 3</b>	<b>9</b>
3.1	Interaction Data Used by MCNP6 . . . . .	9
3.2	Materials Specification – M Card . . . . .	9
3.3	Cross-Section Specification . . . . .	11
3.4	Source Specification . . . . .	11
3.4.1	SI: Source Information Card . . . . .	11
3.4.2	SP: Source Probability Card . . . . .	13
3.5	Examples of Simple Sources . . . . .	13
3.5.1	Point Isotropic Sources . . . . .	13
3.5.2	Isotropic Volumetric Sources . . . . .	15
3.5.3	Line and Area Sources (Degenerate Volumetric Sources) . . . . .	15
3.5.4	Monodirectional and Collimated Sources . . . . .	16
3.5.5	Multiple Volumetric Sources . . . . .	17
3.6	Tally Specifications . . . . .	19
3.6.1	The Surface Current Tally (Type F1) . . . . .	19
3.6.2	The Average Surface Flux Tally (Type F2) . . . . .	20
3.6.3	The Average Cell Flux Tally (Type F4) . . . . .	20
3.6.4	Flux Tally at a Point or Ring Detector (Type F5) . . . . .	21
3.6.5	Tally Specification Cards . . . . .	23
3.6.6	Cards for a Few Optional Tally Features . . . . .	24
3.6.7	Miscellaneous Block 3 Commands . . . . .	25
3.6.8	Short Cuts for Data Entry . . . . .	25
3.7	Running MCNP6 . . . . .	25
<b>4</b>	<b>Variance Reduction</b>	<b>26</b>
4.1	Tally Variance . . . . .	26
4.1.1	Relative Error and FOM . . . . .	27
4.2	Truncation Techniques . . . . .	27
4.2.1	Energy, Time and Weight Cutoff . . . . .	28
4.2.2	Physics Simplification . . . . .	28

4.2.3	Histories and Time Cutoffs . . . . .	30
4.3	Nonanalog Simulation . . . . .	30
4.3.1	Simple Examples . . . . .	30
4.4	MCNP Variance Reduction Techniques . . . . .	31
4.4.1	Geometry Splitting . . . . .	32
4.4.2	Weight Windows . . . . .	33
4.4.3	An Example . . . . .	34
4.4.4	Exponential Transform . . . . .	36
4.4.5	Energy Splitting/Russian Roulette . . . . .	37
4.4.6	Forced Collisions . . . . .	37
4.4.7	Source Biasing . . . . .	37
4.5	Final Recommendations . . . . .	38
<b>5</b>	<b>MCNP Output</b>	<b>38</b>
5.1	Output Tables . . . . .	38
5.2	Accuracy versus Precision . . . . .	39
5.3	Statistics Produced by MCNP . . . . .	40
5.3.1	Relative Error . . . . .	40
5.3.2	Figure of Merit . . . . .	40
5.3.3	Variance of the Variance . . . . .	41
5.3.4	The Empirical PDF for the Tally . . . . .	41
5.3.5	Confidence Intervals . . . . .	43
5.3.6	A Conservative Tally Estimate . . . . .	43
5.3.7	The Ten Statistical Tests . . . . .	44
5.3.8	Another Example Problem . . . . .	44

# A Primer Presenting AN INTRODUCTION TO THE MCNP6 CODE

J. Kenneth Shultis and Amir A. Bahadori

## Introduction

The MCNP<sup>®</sup> Code, developed and maintained by Los Alamos National Laboratory (LANL), is the internationally recognized code for analyzing the transport of neutrons and photons. The current MCNP6 code can simulate the transport of many other radiation particle, namely nine elementary particles ( $\gamma$ ,  $e^-$ ,  $e^+$ ,  $\mu^-$ ,  $\mu^+$ ,  $\nu_e$ ,  $\nu_m$ ,  $\bar{\nu}_e$ ,  $\bar{\nu}_m$ ), 16 composite particles ( $n$ ,  $p$ ,  $\Lambda^0$ ,  $\Sigma^+$ ,  $\Sigma^-$ ,  $\Xi^0$ ,  $\Xi^-$ ,  $\Xi^+$ ,  $\Omega^-$ ,  $\pi^+$ ,  $\pi^-$ ,  $\pi^0$ ,  $K^+$ ,  $K^-$ ,  $K_S^0$ ,  $K_L^0$ ), seven composite antiparticles ( $\bar{n}$ ,  $\bar{p}$ ,  $\bar{\Lambda}^0$ ,  $\bar{\Sigma}^+$ ,  $\bar{\Sigma}^-$ ,  $\bar{\Xi}^0$ ,  $\bar{\Omega}^-$ ), four complex particles ( $d$ ,  $t$ ,  $^3\text{He}$ ,  $\alpha$ ) and several hundred heavy ions ( $Z = 3$  to 92). MCNP is one of the most popular Monte Carlo radiation transport codes.

**Brief Code History** The MCNP series of codes has perhaps the longest history of any Monte Carlo radiation transport code. In the 1950s and 1960s, a number of special purpose Monte Carlo codes, such as MCS, MCN, MCP, and MCG, were developed at LANL. MCS, MCN, and MCG were merged in 1973 to create MCNG, which was merged with the photon code MCP in 1977 to create the first version of MCNP. In 1983, MCNP3 was released for public distribution. Between 1986 and 2011, 19 versions of MCNP were released, each adding additional capability to the code. MCNP6 Beta2 was released in 2012. This version merged MCNP5 with MCNPX (a variant of MCNP5 for high-energy applications). Besides the merging of MCNP5 with MCNPX, 21 new features were incorporated into MCNP6. As a result, MCNP6 has five times the 100k coding lines of MCNP5 and took 12 person-years of effort. In 2023, MCNP 6.3 was released.

Some of the terminology used in the MCNP documentation betrays the code's historical origins. For example, the term *card*, originally an actual punched card, is now just a line of an electronic input file, which is still sometimes referred to as an input *deck*.

**Code Documentation** The documentation for the MCNP6.3 code is contained in several Parts. The current version is MCNP6.3 and Parts I through IV are contained in the technical report *Theory & User's Manual* [Kulesza et al., 2022]. Part I of this report (Chs. 1 and 2) gives the theory behind MCNP6.3. Part II (Chs. 3–8) is the *User's Manual*: Chs. 3 and 4 present, respectively, an overview of MCNP6 and the input to the program. Chapter 5 defines all the commands and options that can be used in the code input; it is essential for both the novice and expert user. Part II ends with Chs. 6–8 which cover advanced features of geometry and tally plotting, a new (to MCNP6.3) alternative plotting capability, and unstructured meshes, respectively. Part III of the Manual (Chs. 9 and 10) contains, respectively, a much more detailed Primer than this humble offering and a large series of examples of the many features of MCNP6.3. These examples are extremely helpful to gain experience with the myriad capabilities of the code. Finally, Part IV comprises six Appendices describing different file formats, utilities, and useful data.

There is another important part of the MCNP6 documentation that is now available only with the MCNP6.3 source code package, namely the *MCNP Developer's Guide*.<sup>1</sup> This restricted manual gives many of the technical details of code; however, it is needed by only MCNP experts who want to alter the code and there is no need for it in this primer.

<sup>1</sup>This restriction is a result of Export Control rules.

The 1078-page MCNP6.3 *Theory & User's Manual* is very comprehensive; thus, it is difficult for new users of the code to distinguish between information vital for learning how to use the code and information needed to use the many hundreds of code options. For this reason, this tutorial document was prepared to introduce the novice with the more basic (and essential) aspects of the MCNP code.

A novice user should first peruse Ch. 1 of the *Theory & User's Manual* to gain an overview of MCNP that summarizes the code's features. Then, a careful reading of this primer describes the preparation of input files, the execution of the code, and the interpretation of results. Here the focus is on so-called *steady-state fixed-source problems*, in which some property of the radiation field, produced by a specified radiation source, is sought at locations or regions of phase space  $(\mathbf{r}, E, \Omega)$ .<sup>2</sup>

After gaining some experience with MCNP, the beginning user should periodically browse through Chapter 2 of the *Theory & User's Manual* to gain a better understanding of the theory behind the many features of MCNP6. Likewise, by periodic skimming Chs. 3–5, an MCNP pupil will become more familiar with all the commands and options that make MCNP such a powerful radiation transport code. In this primer there are several margin notes indicating the page or section in the MCNP6.3 *Theory & User's Manual* (or, for simplicity, the *Manual*) that discuss in more detail the subject being summarized in the primer.

## 1 Structure of the MCNP Input File

An input file consists of a *problem title card* and a maximum of five *blocks* of input cards (lines) arranged as shown to the right. The first and last blocks are optional and often omitted. A *single* blank card separates each block. The input file must not begin with a blank card nor should it end with one. **Block 0** contains options (see §3.3.2.3 of the *Manual*) that are added to the MCNP execution line. The message block starts with the string MESSAGE:. The message block ends with a blank line delimiter before the single required *problem title card*. **Blocks 1** and **2** define the problem geometry. **Block 1** defines all the regions or *cells* of Cartesian  $(x, y, z)$  space. Every point  $(x, y, z)$  must be in one cell or on a cell boundary. **Block 2** defines the surfaces used to form the boundaries of the cells. **Block 3** specifies what MCNP is to do in the simulation. Finally, **block 4** contains command or data cards that are ignored by MCNP but the user wants to keep with the input file. For example, to analyze different shield materials, it is a simple matter to swap material cards between blocks 3 and 4 to analyze a different shield material.

<b>Block 0:</b> exec. options	}	optional
...		
blank delimiter line	}	required
Problem title card		
<b>Block 1:</b> cell cards	}	required
...		
blank delimiter line	}	required
<b>Block 2:</b> surface cards		
...	}	required
blank delimiter line		
<b>Block 3:</b> data cards	}	required
...		
blank delimiter line	}	optional
<b>Block 4:</b> unused cards		
...		

**Input Cards** Input cards (or lines) have a maximum of 128 columns and command mnemonics begin in the first 5 columns. Free field format (one or more spaces separating items on a line) is used and alphabetic characters can be upper or lower case. A continuation line must begin with five blank columns, unless a blank followed by an & is placed at the end of the card to be continued. Tabs are allowed and replaced by blanks to reach the next tab stop (eight columns between tab stops). However, the authors recommend that users refrain from use of tabs for simplicity.

### 1.1 Annotating the Input File

It is good practice to add comments liberally to an input MCNP file so that it is easier for you and others to understand what problem is addressed and how it was solved. A *comment line* begins with C or c followed by a space. Such a line is ignored by MCNP. Alternatively, anything following a \$ sign on a line is ignored. See Fig. 8 on page 35 for a well-annotated MCNP input file.

<sup>2</sup> *Criticality* or *transient* problems, which MCNP6 can also address, are not considered here.

## 1.2 Units Used by MCNP

The units used by MCNP are (1) length in cm, (2) energy in MeV, (3) time in shakes ( $10^{-8}$  s),<sup>3</sup> (4) temperature in MeV (kT), (5) atom density in atoms  $\text{b}^{-1} \text{cm}^{-1}$ , (6) mass density in  $\text{g cm}^{-3}$ , (7) cross sections in b, and (8) deposited energy in jerks  $\text{g}^{-1}$ .<sup>4</sup>

## 2 Geometry Specifications

The cards in Blocks 1 and 2 of the input file define, respectively, the region(s) of 3-D Cartesian space contained in each cell and the surfaces used for the boundaries of the cells. All dimensions are in centimeters (cm). Each of the infinite number of points in the Cartesian space must be in one and only one cell (or be on a boundary surface), i.e., the cells are contiguous and collectively contain all points  $(x, y, z)$ ,  $x, y, z \in (-\infty, \infty)$  in the infinite Cartesian space. There can be no “holes” in the geometry with points that are in no cell. A simulated particle that reaches such a point becomes *lost*. If many particles become lost, then it is likely that there are errors in the MCNP geometry. This is a problem encountered frequently when developing a geometric model, especially by those first learning to use MCNP.

Cells are defined in terms of *surface regions* that lie to one side of first and second degree surfaces. Each surface thus has two surface regions which are often infinite in size. Specifically, cells are defined by Boolean intersections, unions, and compliments of these surface regions. Each cell is filled with a user-defined materials. The union and intersection of two regions A and B are shown by the shaded regions in Fig. 1.

The union operation may be thought of as a logical OR, in that the union of A and B is a new region containing all space either in region A OR region B. The intersection operation may be thought of as a logical AND, in that the result is a region that contains only space common to both A AND B. The complement operator # plays the roll of a logical NOT. For example # (A:B) represents all space outside the union of A and B.

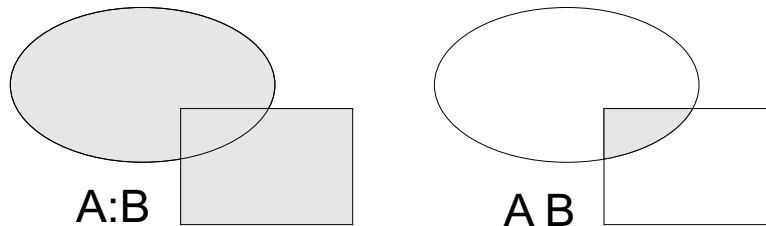


**Figure 1.** Left: the union A:B or “A OR B”. Right: the intersection A B or “A AND B”.

Developing a geometric model for a particular application is usually the most difficult part of preparing the input file and, for a novice, a source of great frustration. After reading the deceptively simple presentation that follows, the introductory discussion in §1.3 should be read. Then to learn more about geometric models study §2.2. Finally, as experience is gained in the development of geometry models, there are many examples provided in §10.1 worthy of careful study.

§1.3, §2.2,  
§10.1

Table 1, taken from the MCNP manual, lists the surfaces used by MCNP to create the geometry

<sup>3</sup>The *shake* is a convenient small time interval (10 ns) used by bomb designers in the once top secret Manhattan Project for use in their experiments and calculations. For example, the time needed to complete one step in a bomb’s chain reaction (or, in nuclear parlance, the *prompt neutron lifetime*) is about  $10^{-8}$  s. The name *shake* comes from the vernacular idiomatic expression “two shakes of a lamb’s tail” to denote a very small time interval.

<sup>4</sup>The *jerk* is another Manhattan Project made-up name defined as  $1 \text{ jerk} = 10^9 \text{ J} = 1 \text{ GJ}$ . One jerk equals  $6.241 \times 10^{21}$  MeV or the explosive energy released by the detonation of 0.238 tonnes of TNT. It should be noted that this nuclear jerk has nothing to do with the jerk of classical mechanics that is a vector and equals the rate of change of the acceleration of an object and so has units of  $\text{cm/s}^3$ . Why the bomb designers recycled the name jerk is a mystery to the authors.

**Table 1.** MCNP Surface Cards [after page 262 of MCNP6.3 *Theory & User's Manual*].

Mnemonic	Type	Description	Equation	Card Entries
P PX PY PZ	plane	general normal to $x$ -axis normal to $y$ -axis normal to $z$ -axis	$Ax + By + Cz - D = 0$ $x - D = 0$ $y - D = 0$ $z - D = 0$	$A B C D$ $D$ $D$ $D$
SO S SX SY SZ	sphere	centered at origin general centered on $x$ -axis centered on $y$ -axis centered on $z$ -axis	$x^2 + y^2 + z^2 - R^2 = 0$ $(x - \bar{x})^2 + (y - \bar{y})^2 + (z - \bar{z})^2 - R^2 = 0$ $(x - \bar{x})^2 + y^2 + z^2 - R^2 = 0$ $x^2 + (y - \bar{y})^2 + z^2 - R^2 = 0$ $x^2 + y^2 + (z - \bar{z})^2 - R^2 = 0$	$R$ $\bar{x} \bar{y} \bar{z} R$ $\bar{x} R$ $\bar{y} R$ $\bar{z} R$
C/X C/Y C/Z CX CY CZ	cylinder	parallel to $x$ -axis parallel to $y$ -axis parallel to $z$ -axis on $x$ -axis on $y$ -axis on $z$ -axis	$(y - \bar{y})^2 + (z - \bar{z})^2 - R^2 = 0$ $(x - \bar{x})^2 + (z - \bar{z})^2 - R^2 = 0$ $(x - \bar{x})^2 + (y - \bar{y})^2 - R^2 = 0$ $y^2 + z^2 - R^2 = 0$ $x^2 + z^2 - R^2 = 0$ $x^2 + y^2 - R^2 = 0$	$\bar{y} \bar{z} R$ $\bar{x} \bar{z} R$ $\bar{x} \bar{y} R$ $R$ $R$ $R$
K/X K/Y K/Z KX KY KZ	cone	parallel to $x$ -axis parallel to $y$ -axis parallel to $z$ -axis on $x$ -axis on $y$ -axis on $z$ -axis	$\sqrt{(y - \bar{y})^2 + (z - \bar{z})^2} - t(x - \bar{x}) = 0$ $\sqrt{(x - \bar{x})^2 + (z - \bar{z})^2} - t(y - \bar{y}) = 0$ $\sqrt{(x - \bar{x})^2 + (y - \bar{y})^2} - t(z - \bar{z}) = 0$ $\sqrt{y^2 + z^2} - t(x - \bar{x}) = 0$ $\sqrt{x^2 + z^2} - t(y - \bar{y}) = 0$ $\sqrt{x^2 + y^2} - t(z - \bar{z}) = 0$	$\bar{x} \bar{y} \bar{z} t^2 \pm 1$ $\bar{x} \bar{y} \bar{z} t^2 \pm 1$ $\bar{x} \bar{y} \bar{z} t^2 \pm 1$ $\bar{x} t^2 \pm 1$ $\bar{y} t^2 \pm 1$ $\bar{z} t^2 \pm 1$ $\pm 1$ used only for 1-sheet cone
SQ	ellipsoid hyperboloid paraboloid	axis parallel to $x$ -, $y$ -, or $z$ -axis	$A(x - \bar{x})^2 + B(y - \bar{y})^2 + C(z - \bar{z})^2$ $+ 2D(x - \bar{x}) + 2E(y - \bar{y})$ $+ 2F(z - \bar{z}) + G = 0$	$A B C D E$ $F G \bar{x} \bar{y} \bar{z}$
GQ	cylinder, cone ellipsoid paraboloid hyperboloid	axis not parallel to $x$ -, $y$ -, or $z$ -axis	$Ax^2 + By^2 + Cz^2 + Dxy + Eyz$ $+ Fzx + Gz + Hy + Jz + K = 0$	$A B C D E$ $F G H J K$
TX TY TZ	elliptical or circular torus. Axis is parallel to $x$ -, $y$ -, or $z$ -axis	$(x - \bar{x})^2/B^2 + (\sqrt{(y - \bar{y})^2 + (z - \bar{z})^2} - A)^2/C^2 - 1 = 0$ $(y - \bar{y})^2/B^2 + (\sqrt{(x - \bar{x})^2 + (z - \bar{z})^2} - A)^2/C^2 - 1 = 0$ $(z - \bar{z})^2/B^2 + (\sqrt{(x - \bar{x})^2 + (y - \bar{y})^2} - A)^2/C^2 - 1 = 0$	$\bar{x} \bar{y} \bar{z} A B C$ $\bar{x} \bar{y} \bar{z} A B C$ $\bar{x} \bar{y} \bar{z} A B C$	
XYZP	surfaces defined by points – see §5.3.2 and §5.3.3 of the <i>Theory &amp; User's Manual</i>			



of a problem.<sup>5</sup>All surfaces are defined in a Cartesian coordinate system. A surface is represented functionally in the form of an equation, as  $f(x, y, z) = 0$ . For example, for a cylinder of radius  $R$  parallel to the  $z$ -axis is defined as  $f(x, y, z) = (x - \bar{x})^2 + (y - \bar{y})^2 - R^2$ , where the cylinder's axis is parallel to the  $z$ -axis and passes through the point  $(\bar{x}, \bar{y}, 0)$ . The MCNP input line for such a surface, which is denoted by the mnemonic C/Z (or c/z, since MCNP is case insensitive), is

```
1 C/Z 5 5 10 $ a cylindrical surface parallel to z-axis
```

defines surface 1 as an infinitely long cylindrical surface parallel to  $z$ -axis with radius of 10 cm and whose axis passes through the point  $(x = 5 \text{ cm}, y = 5 \text{ cm}, z = 0)$ . Note that the length of the cylinder is infinite. Note also the *in-line comment*, introduced by the \$ symbol.

Every surface has a “positive” side and a “negative” side. These directional senses for a surface are defined formally as follows: any point at which  $f(x, y, z) > 0$  is located in the positive sense (+) to the surface, and any point at which  $f(x, y, z) < 0$  is located in the negative sense (−) to the surface. These are the two *surface regions* associated with every surface. For example, a region within a cylindrical surface is negative with respect to the surface and a region outside the cylindrical surface is positive with respect to the surface.

## 2.1 Cells – Block 1

We illustrate how surfaces and Boolean logic are used to define cells by considering a simple example of a cylindrical storage cask whose wall and ends are composed of iron 1-cm thick. Inside and outside the cask are void regions. Suppose the outer cylindrical surface is that used in the illustration in the previous section. The geometry for this problem is shown in Fig. 2.

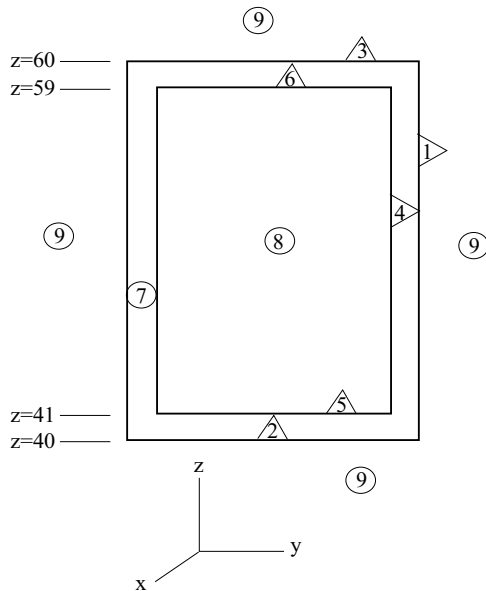


**Figure 2.** Geometry for a simple cylindrical cask. Numbers in triangles are surface identification numbers and the triangle points to the (+) side of the surface. Numbers in circles define the cell identification number. The axis of the cask passes through the point  $(x = 5 \text{ cm}, y = 5 \text{ cm})$  and the cask outer radius is 10 cm.

To define the inside surface of the cask, we need another cylinder inside and concentric with the first cylinder but with a radius smaller by 1 cm. We shall call this smaller cylindrical surface number 4, so that the surface definition lines in the input file for these two cylinders are

```
1 C/Z 5 5 10 $ outer cylindrical surface
4 C/Z 5 5 9 $ inner cylindrical surface
```

To define the base and top of the cask, planes perpendicular to the  $z$ -axis are needed at locations  $z = 40 \text{ cm}$  and  $z = 60 \text{ cm}$ , respectively. Similarly, to define the base and top of the inner cavity

<sup>5</sup>Because surfaces must be defined before the cells can be specified in terms of the bounding surfaces, we discuss Block 2 before Block 1. Why MCNP requires the input of cell definitions before the bounding surface definitions is unknown to the authors. In practice, one creates block 2 before block 1.

of the cask two more planes perpendicular to the  $z$ -axis are needed at  $z = 41$  cm and  $z = 59$  cm. These four planes are defined by

```

2  PZ  40          $ base of cask
3  PZ  60          $ top of cask
5  PZ  41          $ base of inner cavity
6  PZ  59          $ top of inner cavity

```

The surface definition cards (or input lines) can appear in any order in Block 2 of the input file. Each surface must have a unique positive integer identifier ( $< 10^8$ ). Here the surface numbers are 1, 2, 3, 4, 5, and 6. They need not be ordered as in this example but they must begin in columns 1–5.

With the problem surfaces defined, we now begin to define the volumes or cells which must fill all  $(x, y, z)$  space. These cell definition cards comprise the content of Block 1 of the input file. First, we define the inner void of the cask as cell 8. This volume is negative with respect to surface 4, positive with respect to the plane 5, and negative with respect to plane 6. Thus, cell 8 is defined as

```

8  0  -4 5 -6      IMP:N=0 IMP:P=1  $ inner cask void

```

The first number on a cell definition card is the cell identifier (any positive integer  $< 10^8$ ) and must begin in columns 1–5. Here the second entry 0 denotes that the cell is filled by a void, and -4 5 -6 indicate that all points in cell 8 are inside the cylinder 4 AND are above plane 5 AND are below plane 6. region. The last two IMP specifications define the *importance* of this region to neutrons (N) and (P). Neutrons in this cell have zero weight and photons have unit weight (i.e., we assume only photon sources are stored in the cask). We’ll discuss importances later. The order of surfaces in an intersection string is arbitrary. Thus, we could have defined cell 8 by intersection of surfaces -6 -4 5.

Now consider the iron shell of the cask. Suppose this cell is given 7 as its id number and consists of material 5, as yet to be defined, with density  $7.86 \text{ g cm}^{-3}$ . Space within this cell is negative with respect to surface 1, positive with respect to surface 2 and negative with respect to surface 3 AND also cannot be inside the void or cell 8. This cell can thus be defined as

```

7  5 -7.86  -1 2 -3 #8  IMP:N=0 IMP:P=1  $ iron cask shell

```

Although the *complement operator #* (for NOT) is often a convenient way to exclude an inner region, this operator often reduces the efficiency of MCNP. In fact, theoretically one never has to use #. The region outside cell 8 can be defined by the union string (4:6:-5) and the definition of cell 7 can be equivalently defined as

```

7  5 -7.86  -1 2 -3 (4:6:-5)  IMP:N=0 IMP:P=1  $ iron cask shell

```

Now suppose that cells 7 and 8 describe all space of interest for radiation transport. In other words, suppose that all photons passing outside the outer surface of the finite cylinder may be killed, i.e., their path tracking can be ended. One still needs to assign this space to a cell. Further by setting the photon importance in this cell to zero, any photon entering is killed. This “graveyard” cell, say cell 9, is the union of all regions positive with respect to surfaces 1 and 3 and negative with respect to surface 2. Hence the graveyard is defined by

```

9  0          1:3:-2          IMP:N=0 IMP:P=0  $ graveyard

```

The graveyard could also be defined by using the complement operator and by specifying that the kill zone is all space outside the union of cells 7 and 8, namely

```

9  0          #(7:8)          IMP:N=0 IMP:P=0  $ graveyard

```

Note that the second entry on this cell card is zero, indicating a vacuum and that the photon importance is set to zero.

## 2.2 Macrobodies

§5.3.4

MCNP has an alternative way to define cells and surfaces through the use of macrobodies. These macrobodies can be mixed with the standard cells and surfaces and are defined in Block 2. For example, the command in Block 2

**Table 2.** Macrobodyes available in MCNP.

Mnemonic	Type of body
BOX	arbitrarily oriented orthogonal box (90° corners)
RPP	rectangular parallelepiped (surfaces parallel to axes)
SPH	sphere
RCC	right circular cylinder
RHP or HEX	right hexagonal prism
REC	right elliptical cylinder
TRC	truncated right-angle cone
ELL	ellipsoid
WED	wedge
ARB	arbitrary polyhedron

```
15 RCC 1 2 5 0 0 50 10 $ right circular cylinder
```

defines a right circular cylinder with the following properties: the center of the base is at (1,2,5); the height is 50 cm and the axis is parallel to the  $z$ -axis; the radius is 10 cm; and the macrobody has 15 as its identifier.

The macrobodyes available in MCNP are shown in Table 2. MCNP automatically decomposes the macrobody surface into surface equations and the facets are assigned identifying numbers according to a predetermined sequence. The assigned surface number consists of the macrobody identifier number follow by a decimal point and an integer 1, 2, . . . . For example in the RCC example above, the cylindrical surface has the identifier 15.1, the plane of the top is 15.2, and the plane of the base is 15.3. These facet surfaces can be used for anything standard surfaces are used for, e.g., tallies, other cell definitions, source definitions, etc.

The definition of a macrobody can require many parameters. Here we give the details for three of the most useful macrobodyes.

**BOX Arbitrarily oriented orthogonal box:** This body is defined by four vectors:  $\mathbf{v}$  defining a corner of the box and three orthogonal vectors  $\mathbf{a}$ ,  $\mathbf{b}$ , and  $\mathbf{c}$  defining the length and direction of the sides from the specified corner. The syntax is §5.3.4.1

```
BOX v_x v_y v_z a_x a_y a_z b_x b_y b_z c_x c_y c_z
```

The facet suffixes are: .1/.2 plane perpendicular to the end/beginning of  $\mathbf{a}$   
 .3/.4 plane perpendicular to the end/beginning of  $\mathbf{b}$   
 .5/.6 plane perpendicular to the end/beginning of  $\mathbf{c}$

**RPP Rectangular parallelepiped:** This orthogonal box has sides perpendicular to the coordinate axes. This body is defined by the range each side has along its parallel axis. The syntax is §5.3.4.2

```
RPP x_min x_max y_min y_max z_min z_max
```

The facet suffixes are: .1/.2 plane  $x_{\max}/x_{\min}$ ; .3/.4 plane  $y_{\max}/y_{\min}$ ; .5/.6 plane  $z_{\max}/z_{\min}$ .

**RCC right circular cylinder:** A right cylinder is specified by a vector  $\mathbf{v}$  giving the center of the base, a vector  $\mathbf{h}$  defining the axis and height of the cylinder, and the radius  $R$ . The syntax is §5.3.4.4

```
RCC v_x v_y v_z h_x h_y h_z R
```

The facet suffixes are: .1 cylindrical surface; .2/.3 plane normal to the end/beginning of  $\mathbf{h}$ .

NOTE: *The space inside a macrobody has a negative sense with respect to all the macrobody's bounding surfaces.* The space outside the bounding surfaces has a positive sense to the macrobody.

More important to remember is that the sense of a macrobody's bounding surfaces or facets is the sense assigned to it by the macrobody and the facet surface retains this sense even if it appears in other cell definitions. For example, the base of the RCC cylinder discussed above is a plane normal to the  $z$ -axis with intercept of 5 cm and has the identifier 15.3. The space with  $z > 5$  has a *negative* sense to this surface because this space is towards the interior of the cylinder. The space for  $z < 5$  has a positive sense because this region is outside the macrobody. This sense convention for macrobody surfaces is different from the sense convention of standard surfaces. The surface 15.3 is equivalent to a plane surface 16 defined as 16 PZ 5, but space with  $z > 5$  has a positive sense with respect to surface 16 while it has a negative sense for surface 15.3!

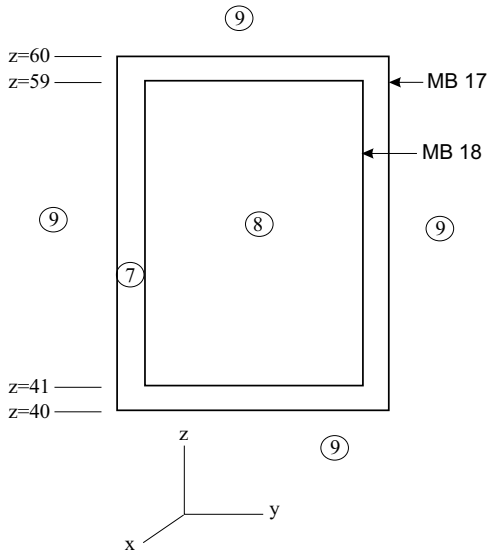


**Figure 3.** Geometry for a simple cylindrical cask. Two macrobody right cylinders are used to define the inside and outside surfaces of the cask and numbers in circles are the cell identification number. As before, the axis of the cask passes through the point  $(x = 5 \text{ cm}, y = 5 \text{ cm}, z = 0)$

The use of macrobodies can greatly ease the specification of a problem's geometry. We illustrate this by returning to the simple cask problem considered in the previous section. Rather than define 6 surfaces to form the cask, we use two nested cylinder macrobodies. The subsequent Boolean logic used to define the three cells now becomes considerably simpler. For the geometry shown in Fig. 3, the input geometry specification becomes

```
Use of macrobodies for cask problem
c ***** BLOCK 1 -- cells
8 0 -18 IMP:P,N=1 $ inside the cask
7 5 -7.86 18 -17 IMP:P,N=1 $ cask iron shell
9 0 17 IMP:P,N=0 $ void outside cask

c ***** BLOCK 2 -- surfaces/macrobody
17 RCC 5 5 40 0 0 20 10 $ outer cylinder
18 RCC 5 5 41 0 0 18 9 $ inner cylinder
```

Cell 8 is simply all the space inside macrobody 18 and is denoted by -18. Cell 7 is all the space inside macrobody 17 and outside macrobody 18, namely 18 -17. These cell definitions are considerably simpler than those based on the intersections and unions of the six standard surfaces used in the previous definition of this cask.

### 2.2.1 Unstructured Meshes

The use of macrobodies and the ability to construct geometric regions from Boolean operations on bounding surfaces gives MCNP a very powerful constructive solid geometry (CSG) capability. It has been extensively tested and verified. However for complex geometries the CSG approach for specifying a problem geometry is labor intensive and susceptible to errors which are often hard to debug.

New to MCNP6 is the ability to use an unstructured mesh (UM) to define a problem geometry. This alternative to CSG is an exciting development but one that is still evolving and one novice MCNP users should ignore until they have gained some experience with MCNP.

### 3 Data Specifications – Block 3

This block of input cards defines the type of particles, problem materials, radiation sources, how results are to be scored (or tallied), the level of detail for the physics of particle interactions, variance reduction techniques, cross section libraries, the amount and type of output, and much more. In short, the third input block provides almost all a problem’s specifications other than the geometry.

The 60 or so different commands cards and the sometimes many KEYWORDS (options) for the commands are extensively discussed in Ch. 5 of the *Manual*. Here some necessary background and a few of the more commonly used commands for simple problems are briefly reviewed.

#### 3.1 Interaction Data Used by MCNP6

The nuclear data needed by MCNP6 to describe the interactions of particles with the ambient medium as they transported through the problem geometry are provided by (1) pointwise cross-section data and other extensive data tables and/or (2) various nuclear physics models, used primarily for high-energy particles ( $> 150$  MeV). Unlike many other transport codes, all this nuclear data is an integral part of the MCNP code. The various libraries and data tables distributed with MCNP6.3 are listed in LA-UR-17-20709 (Conlin, 2017). Relevant nuclear data are now distributed separately from the MCNP code to decouple updates between the two. Nuclear data for use with MCNP can be obtained from <https://nucldata.lanl.gov/>.

§2.3

For neutrons with energies up to 150 MeV, the comprehensive ENDF/B-VII data files are composed of pointwise (continuous-energy) interaction data and secondary-particle production data, for a few hundred target isotopes.<sup>6</sup> Proton interaction data for 48 isotopes are provided for energies from 1 to 150 MeV. Photon and electron/positron data are included for energies of 1 eV to 100 GeV and from 10 eV to 1 GeV, respectively. Photonuclear data for 157 isotopes are included for photon energies up to 150 MeV. Above the maximum energies of these data tabulations, and for all hadrons, interaction physics are based on theoretical models with empirical corrections.

§2.3.1, §2.3.6

#### 3.2 Materials Specification – M Card

Specification of materials filling the the various cells in an MCNP calculation uses an M card in block 3 for each material. This card specifies (a) defining a unique material number (a positive integer  $< 10^8$ ), (b) the elemental (or isotopic for neutrons) composition, and (c) the libraries of cross section and data tables to be used. The ZAIID number ZZZAAA identifies a specific nuclide or element. For example, elemental uranium is 092000, or simply 92000, whereas the isotope  $^{235}_{92}\text{U}$  has a ZAIID of 92235.

§5.6

Note that mass density is not specified here. Instead, density is specified on the cell definition card. This permits one material to appear at different densities in different cells. Suppose that the first material to be identified in problem input is (light) water and that only gamma-ray transport is of interest. Comment cards (cards beginning with C or c) may be used for narrative descriptions. In the following card images, the designation M21 refers to material 21. For a compound, unnormalized (stoichiometric) atomic fractions may be used. For example,

```

c -----
c WATER for gamma-ray transport (by atom fraction)
c -----

```

<sup>6</sup>Some discrete reaction tables in which the cross sections are averaged over 262 groups are also available for use on computers with very limited memory. These tables should be avoided.

```

M21  1000  2          $ elemental H and atomic abundance
      8000  1  PLIB=04p $ elemental O and atomic abundance

```

The designations 1000 and 8000 identify elemental hydrogen, atomic number  $Z = 1$ , and elemental oxygen ( $Z = 8$ ). The three zeros in each designation are place holders for the atomic mass number, which would be required to identify specific isotopes of the element and which, generally, are required for neutron transport, as described later. For gamma ray and electron transport, one needs to specify only the atomic number. The keyword `PLIB=04p` says the 04p photon library is to be used. Alternatively one could omit `PLIB=04p` and just append it to the ZAIDs, i.e., `1000.04p` and `8000.04p`.

For compounds or mixtures, composition may alternatively be specified by mass fraction, indicated by a minus sign, as follows:

```

c -----
c WATER for gamma-ray transport (by mass fraction)
c -----
M21  1000.04p  -0.11190  $ elemental H mass fraction
      8000.04p  -0.88810  $ elemental O mass fraction

```

Note mass and atom fractions need not sum to unity; MCNP will normalize them.

For neutron transport problems, often specific isotopes of an element must be specified. If neutron cross sections for an element composed of its isotopes in their naturally occurring abundances is desired, then sometimes the ZAID can be specified as `ZZZ000`. Note, such elemental neutron cross section sets are old and not available for all elements. Usually one must list all of the important isotopes. As an example, light water for neutron problems could be defined as

```

c -----
c WATER for neutron transport (by mass fraction)
c      (ignore H-2, H-3, O-17, and O-18)
c -----
M21  1001.80c  -0.11190  $ H-1 and mass fraction
      8016.80c  -0.88810  $ O-16 and mass fraction

```

Here 1001 and 8016 provide atomic number and atomic mass designations, in the form of the ZAID numbers. The `80c` designation identifies the ENDF/B-VII.1 cross section compilation. Other compilations distributed with MCNP6.3 are given by Conlin [2017]. There is no hard and fast rule as to which neutron library is “best” (see also Section 3.2 below).

§2.3.1

When hydrogen is molecularly bound in water, either in pure form or as a constituent in some other material, the binding affects energy loss in collisions experienced by slow neutrons. For this reason, special cross-section data treatments are provided that take binding effects into account. To use this special treatment, an additional MT card is required, as shown below.

§5.6.2

```

c -----
c WATER for neutron transport (by mass fraction)
c      (ignore H-2, H-3, O-17, and O-18)
c      Specify S(alpha,beta) treatment for binding effects
c -----
M21  1001.80c  -0.11190  $ H-1 and mass fraction
      8016.80c  -0.88810  $ O-16 and mass fraction
MT21  lwtr.20t          $ light water at 293.6 K

```

Without the MT card, hydrogen would be treated as if it were a monatomic gas. With the  $S(\alpha, \beta)$  treatment, fast neutrons slowing down to thermal energies will develop a Maxwellian energy distribution with the specified temperature. Treatment of binding effects for other nuclides, materials and temperatures are also provided [Conlin et al. 2017].

### 3.3 Cross-Section Specification

Neutron interactions and the history and many sources of cross-section data tables are described in Section 2.3.1 of the the MCNP6 *Manual*. A comprehensive list of cross section compilations in the ACE format distributed with MCNP6 is provided by Conlin and the LANL Nuclear Data Team [2017]. This 500-page Technical Report replaces the infamous Table G2 of Appendix G to Vol. I for MCNP5 and MCNP4. Specification of a particular cross-section compilation depends somewhat on the nature of the problem being solved and on the data available to the user. Not all cross section sets are available to all users. For users obtaining data through the Radiation Safety Information Computation Center (RSICC), a common choice would be the 80c library, which was derived from the ENDF/B-VII.1 evaluated nuclear data files for room-temperature, Doppler broadening of neutron cross sections. For Doppler broadening at other temperatures, other libraries are also available.

In a few instances, neutron cross sections are available for elements with naturally occurring atomic abundances. For example, natural chromium can be specified as 24000.50c. However, elemental neutron cross sections are rare and, for the very few such libraries available, the underlying data are old. Generally, it is necessary for the user to define a natural element as a combination of the natural occurring isotopes. Even then, data for nuclides with small (<0.1%) isotopic abundances are often not available and the trace isotopes must be neglected (as was done in the previous section for light water).

### 3.4 Source Specification

The source and the radiation particles it emits in a fixed-source MCNP problem are specified by the `SDEF` command. The `SDEF` command has many keywords or parameters that are used to define *all* the characteristics of all sources in the problem. The `SDEF` command with its many keywords and their possible values is one of the more complex MCNP commands and is capable of producing an incredible variety of sources — all with a single `SDEF` command. And only one `SDEF` card is allowed in an input file!

§5.8.1 to  
§5.8.6

On the `SDEF` card values of appropriate keywords in Table 4 are entered, if other than the default values, that are needed to characterize a particular source. The = sign is optional, so that `PAR=1` is equivalent to `PAR 1`. Values of variables can be specified at three levels: (1) explicitly (e.g., `ERG=1.25`), (2) with a *distribution* number (e.g., `ERG=d5`), and (3) as a function of another variable (e.g., `ERG=Fpos`). Specifying variables at levels 2 and 3 requires the use of two ancillary source cards: the `SI` (source information) card and the `SP` (source probabilities) card.<sup>7</sup>

#### 3.4.1 SI: Source Information Card

This card tells MCNP how  $K$  values  $i_1, \dots, i_K$  about a source variable (e.g., energies of photon spectral lines) are to be interpreted. The form of the `SI` card is

`SIn option  $i_1, \dots, i_K$`

where `n` is the distribution number specified on the `SDEF` card. The four possible options are listed below

§5.8.2

- `option = H`  $i$  values are monotonically increasing histogram bin upper boundaries
- `option = L`  $i$  values are discrete source variable values (e.g., cell numbers or energies of photon spectrum lines).
- `option = A`  $i$  values are points where a probability density is defined. Entries must be monotonically increasing, with the lowest and highest values defining the range of the variable.
- `option = S`  $i$  values are distribution numbers.

<sup>7</sup>Two other ancillary source cards are available for more advanced applications: the `SB` (source biasing) card and the `DS` (source dependent) distribution card.

**Table 3.** MCNP6 particle identifiers and the minimum tracking energy for the more commonly used particles. Data for other leptons, baryons and mesons are given in Table 4.3 of the *Manual*.

PAR	Name	MCNP Symbol	Low-E Cutoff (MeV)	Default Cutoff (MeV)	PAR	Name	MCNP Symbol	Low-E Cutoff (MeV)	Default Cutoff (MeV)
1	neutron (n)	N	0.0	0.0	31	deuteron (d)	D	$10^{-3}$	2.0
2	photon ( $\gamma$ )	P	$10^{-6}$	$10^{-3}$	32	triton (t)	T	$10^{-3}$	3.0
3	electron ( $e^-$ )	E	$10^{-5}$	$10^{-3}$	33	helion ( $^3\text{He}$ )	S	$10^{-3}$	3.0
8	positron ( $e^+$ )	F	$10^{-3}$	$10^{-3}$	34	alpha particle ( $\alpha$ )	A	$10^{-3}$	4.0
9	proton ( $e^+$ )	H	$10^{-3}$	1.0	37	heavy ion ( $^A_Z\text{X}$ )	#	$10^{-3}$	5.0

**Table 4.** Source keywords for the SDEF command.

Variable	Meaning	Default
CEL	cell	determined from the position of the particle, and possibly the particle's flight direction if the position is on a cell surface.
SUR	surface	SUR=0 means cell (volume) source
ERG	kinetic energy (MeV)	14 MeV
DIR	$\mu$ , the cosine of the angle between VEC and particle flight direction. The azimuthal angle is always sampled uniformly in $[0, 2\pi]$ .	Volume case: $\mu$ is sampled uniformly in $[-1, 1]$ (isotropic). Surface case: $p(\mu) = 2\mu$ for $\mu \in [0, 1]$ (cosine distribution).
VEC	reference vector for VEC	Volume case: required unless isotropic. Surface case: vector normal to the surface with sign determined by NRM.
NRM	sign of the surface normal	+1
POS	reference point for positioning sampling	0, 0, 0
RAD	radial distance of the position from POS or AXS	0
EXT	Cell case: distance from POS along AXS. Surface case: cosine of angle from AXS	0
AXS	reference vector for EXT and RAD	no direction
X	x-coordinate of position	X=0
Y	y-coordinate of position	Y=0
Z	z-coordinate of position	Z=0
CCC	cookie-cutter cell	no cookie-cutter cell
ARA	area of surface (required only for direct contributions to point detectors from a plane surface source)	none
WGT	particle weight	1
EFF	reference efficiency criterion for position sampling	0.01
PAR	type of particle source emits. Many choices e.g., cosmic ray, background, particles from radioactive decay.	particle with smallest IPT value on MODE card: N=1, P=2, E=3, ...



### 3.4.2 SP: Source Probability Card

This card gives the probabilities for each item on the corresponding SI card. It has the two forms

SPn option  $p_1, \dots, p_K$       and      SPn -f a b

where n is the distribution number specified on the SDEF card and the option letter specifies how the  $p_i$  are to be interpreted according to the following list (only the 5 most frequently used options are listed here). §5.8.3

option omitted	the same as D for an H or L distribution on the SI card or a probability density for an A distribution on the SI card.
option = D	$p_i$ values are bin probabilities for an H or L distribution on the SI card. (Default value).
option = C	$p_i$ values are cumulative bin probabilities for an H or L distribution on the SI card.
option = V	$p_i$ values are for CEL distributions; the probability is proportional to a cell's volume ( $\times p_i$ if the $p_i$ are present)
option = -f	a negative integer specifies the use of a built-in function with parameter values a and possibly b. See §5.8.3.1 of the <i>Manual</i>

## 3.5 Examples of Simple Sources

Often MCNP problems involve fairly simple fixed sources that for a novice can be challenging to implement in MCNP. The documentation for MCNP5 and earlier versions devoted only a few exceptionally terse pages to the SDEF and ancillary cards. The few source examples in the examples chapter were far too complex for an MCNP beginner to understand and use to create a simple source, which was a primary motivation for our Primer on MCNP5. With the simple examples in our first MCNP Primer, our students were able to start using MCNP with greater ease.

With the advent of MCNP6(v.1), the user's manual has greatly expanded the discussion about sources until the latest version for MCNP6.3 [Kulesza et al., 2022] devotes almost 60 very understandable pages and many "simple" examples to the subject. Kudos to the authors! However, many of these simple examples illustrate advanced features not covered in this primer. Presented below are some even simpler source examples. These are designed to help the novice MCNP user model many common source situations, rather than demonstrate the subtleties or alternative syntax for keywords and options of the SDEF card. §5.8

Once users have gained confidence with simple source models, they should begin studying the often complicated source examples given in Chapter 10 of the *Manual*. From periodic perusals of §5.8 and §10.3 of the *Manual* one usually gains new insight into the robustness of the SDEF command. It is probably the most powerful, complex, and flexible of all the MCNP commands, and consequently, the most difficult one to master. §10.3

Finally, a cautionary word learned from experience. When you develop a new source model, always check and recheck that source particles are truly being generated where you think they should be and are born with the correct energies and directions of travel. HINT: place the VOID card and the PRINT 110 statement somewhere in block 3 of the input file. The PRINT 110 causes the starting locations, directions, and energies of the first 50 particles to be printed to the output file. Examine this output table to convince yourself that particles are being generated as you expect.

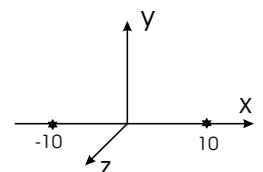
### 3.5.1 Point Isotropic Sources

#### Two Point Isotropic Sources at Different Positions

```

c ----- Two point, isotropic, 1-MeV, photon sources on x-axis
SDEF ERG=1.00 PAR=2 POS=d5      $ energy, particle type, location
SI5 L  -10 0 0  10 0 0          $ (x,y,z) coords of the two pt sources
SP5     .75     .25             $ relative strengths of each source

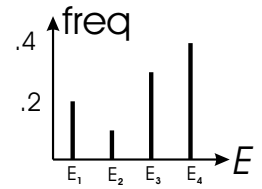
```



### Point Isotropic Source with Discrete Energy Photons

```

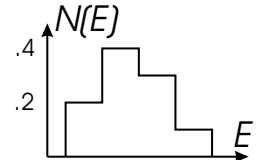
c ----- Point isotropic source with 4 discrete photon energies
SDEF POS 0 0 0   ERG=d1  PAR=2
SI1 L .3 .5 1. 2.5  $ the 4 discrete energies (MeV)
SP1  .2 .1 .3 .4  $ frequency of each energy
    
```



### Point Isotropic Source with a Histogram of Energies

```

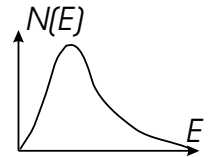
c ----- Point isotropic photon source with 4 histogram energy bins
c          NOTE: range of first E-bin is (-infty,E1) with prob p1=0
SDEF POS 0 0 0   PAR=P   ERG=d1  $ position, part type, E distn
SI1 H .1 .3 .5 1. 2.5  $ histogram upper boundaries
SP1 D 0 .2 .4 .3 .1  $ probabilities for each bin
    
```



### Point Isotropic Source with a Continuum of Energies

```

c ----- Point isotropic neutron source with Maxwellian energy spectrum
SDEF POS 0 0 0   PAR=N   ERG=d1  $ position, particle type, energy
SP1 -2 0.5  $ Maxwellian spectrum (2) with temp a=0.5 MeV
    
```

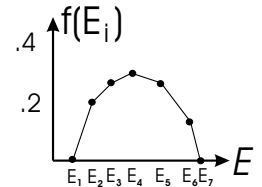


### Point Isotropic Source with Tabulated Energy Distribution

#### (a) Horizontal Input

```

c ----- Isotropic proton source w cont.-E PDF listed at discrete Es
SDEF POS 0 0 0   PAR=H   ERG=d7  $ position, particle type, E distn
SI7 A 1 2 3 4 5.5 7.0 7.5  $ tabulated energies E1 ... E7
SP7 D 0 .2 .27 .3 .28 .18 0  $ tabulated PDF values f(Ei)
    
```



#### (b) Vertical Input

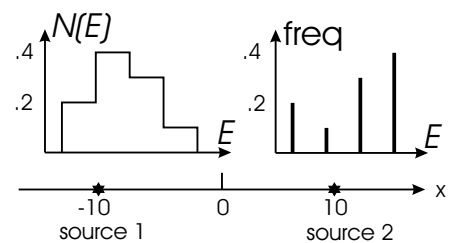
```

c ----- Isotropic proton source w cont.-E PDF listed at discrete Es
SDEF POS 0 0 0   PAR=H   ERG=d7  $ position, particle type, E distn.
c ----- use vertical input for PDF -- easiest if many Ei
#      SI7      SP7      $ # sign indicates start of vertical input
      A        D
      1.0      0.0      $ E1 f(E1) start of PDF
      2.0      .20      $ E2 f(E2)
      3.0      .27      $ E3 f(E3)
      4.0      .30      $ E4 f(E4)
      5.5      .28      $ E5 f(E5)
      7.0      .18      $ E6 f(E6)
      7.5      0.0      $ E7 f(E7) end of PDF and vertical input
    
```

### Two Point Sources with Different Energy Distributions

```

c --- 2 pt iso sources: src 1 (4-bins) src 2 (4 discrete Ei)
SDEF PAR=2 POS=d1 ERG FPOS d2
SI1 L -10 0 0 10 0 0  $ coords of srcs on x-axis
SP1  .4 .6  $ rel strengths of sources
DS2 S 3 4  $ energy distributions
SI3 H .1 .3 .5 1. 2.5  $ E bin limits src 1
SP3 D 0 .2 .4 .3 .1  $ bin prob for src 1
SI4 L .3 .5 .9 1.25  $ discrete Ei for src 2
SP4  .20 .10 .30 .40  $ rel freq for src 2
    
```



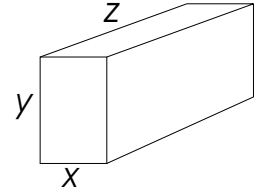
### 3.5.2 Isotropic Volumetric Sources

#### Rectangular Parallelepiped Parallel to Axes

```

c --- volumetric monoenergetic source inside a rectangular parallelepiped
SDEF X=d1 Y=d2 Z=d3  ERG=1.25  PAR=2
SI1 -10. 10.          $ x-range limits for source volume
SP1  0  1             $ uniform probability over x-range
SI2 -15. 15.          $ y-range limits for source volume
SP2  0  1             $ uniform probability over y-range
SI3 -20. 20.          $ z-range limits for source volume
SP3  0  1             $ uniform probability over z-range

```



#### Source in a Complex Cell: Enclosing Parallelepiped Rejection Method

```

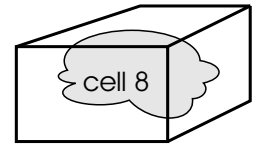
c --- Cell 8 is some complex cell in which a monoenergetic isotropic
c      volumetric source exists. A rectangular parallelepiped envelops
c      this cell (MCNP does NOT check this!). Points, randomly picked
c      in the rectangular parallelepiped, are accepted as source points
c      only if they are inside cell 8.

```

```

c
SDEF X=d1 Y=d2 Z=d3  ERG=1.25  PAR=2  CEL=8
c NOTE: source parallelepiped is larger than cell 8, and hence
c      source positions sampled outside cell 8 are rejected.
SI1 -12. 12.          $ x-range limits for source volume
SP1  0  1             $ uniform probability over x-range
SI2 -11. 11.          $ y-range limits for source volume
SP2  0  1             $ uniform probability over y-range
SI3 -13. 13.          $ z-range limits for source volume
SP3  0  1             $ uniform probability over z-range

```



#### Source in a Complex Cell: Enclosing Sphere Rejection Method

```

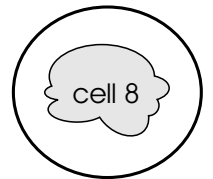
c --- Cell 8 is some complex cell in which a monoenergetic isotropic
c      volumetric source exists. A sphere envelops this cell (MCNP
c      does NOT check this!). Points, randomly picked in the sphere,
c      are accepted as source points only if they are inside cell 8.

```

```

c
SDEF POS=0 0 0  RAD=d1  CEL=8
SI1  0 20.          $ radial sampling range: 0 to Rmax (=20cm)
SP1 -21 2           $ weighting for radial sampling: here r^2

```



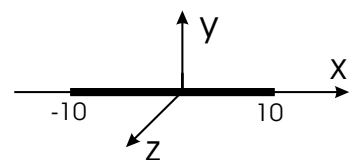
### 3.5.3 Line and Area Sources (Degenerate Volumetric Sources)

#### Line Source (Degenerate Rectangular Parallelepiped)

```

c --- Line monoenergetic photon source lying along x-axis
c      This uses a degenerate Cartesian volumetric source.
c
SDEF POS=0 0 0  X=d1 Y=0 Z=0  PAR=P  ERG=1.25
SI1 -10 10       $ Xmin to Xmax for line source
SP1 -21 0        $ uniform sampling on line Here x^0

```

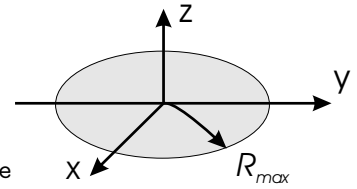


### Disk Source (Degenerate Cylindrical Source)

```

c --- disk source in x-y plane centered at the origin.
c     This is a degenerate cylindrical volume source.
c
SDEF POS 0 0 0  AXS 0 0 1 EXT 0  RAD d1  PAR P  ERG 1.25
SI1  0  11      $ radial sampling range: 0 to Rmax
SP1 -21  1      $ radial sampling weighting: r^1 for disk source

```

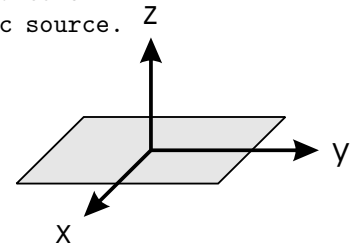


### Plane Source (Degenerate Rectangular Parallelepiped)

```

c --- rectangular plane source centered on the origin and perpendicular
c     to the y-axis. This uses a degenerate Cartesian volumetric source.
c
SDEF POS=0 0 0  X=d1 Y=d2 Z=0  PAR=P  ERG=1.25
SI1 -10 10      $ sampling range Xmin to Xmax
SP1  0  1      $ weighting for x sampling: here constant
SI2 -15 15      $ sampling range Ymin to Ymax
SP2  0  1      $ weighting for y sampling: here constant

```

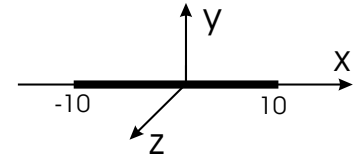


### Line Source (Degenerate Cylindrical Source)

```

c --- line source (degenerate cylindrical volumetric source)
SDEF pos=0 0 0  axs=1 0 0 ext=d1 rad=0  par=2 erg=1.25
SI1  -10 10      $ axial sampling range: -X to X
SP1  -21 0      $ weighting for axial sampling: here constant

```



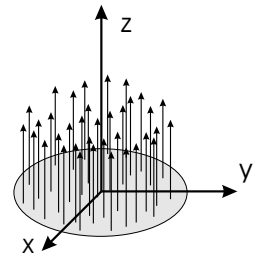
## 3.5.4 Monodirectional and Collimated Sources

### Monodirectional Disk Source

```

c --- Disk source perpendicular to z-axis uniformly emitting
c     1.2-MeV neutrons monodirectionally in the +ve z-direction.
c
SDEF POS=0 0 0  AXS=0 0 1 EXT=0  RAD=d1  PAR=1  ERG=1.2
      VEC=0 0 1  DIR=1
SI1  0  15      $ radial sampling range: 0 to Rmax (=15cm)
SP1 -21  1      $ radial sampling weighting: r^1 for disk

```

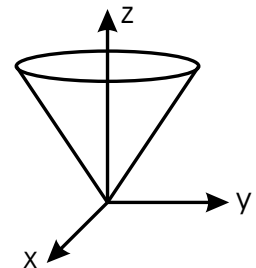


### Point Source Collimated into a Cone of Directions

```

c --- Point isotropic 1.5-MeV photon source collimated into
c     an upward cone. Particles are confined to an upward
c     (+z axis) cone whose half-angle is acos(0.9) = 25.8
c     degrees about the z-axis. Angles are with respect to
c     the vector specified by VEC
c
SDEF POS=0 0 0  ERG=1.25  PAR=2  VEC=0 0 1  DIR=d1
SI1  -1  0.9  1      $ histogram for cosine bin limits
SP1  0 0.95  0.05    $ frac. solid angle for each bin
SB1  0.  0.  1.      $ source bias for each bin

```



With this conical source, tally normalization is per source particle in  $4\pi$  steradians. To normalize the tally per source particle in the cone, put `WGT=1/fsa2` on the SDEF card, where `fsa2` is the fraction solid angle of the cone (0.05 in the above example).

## Biasing the Source Emission Direction

The above conical collimation trick can also be used to preferentially bias the emission of particles in certain directions. The SIn entries are the upper bin cosine limits  $\mu_i \equiv \cos \theta_i$  in ascending order. The first entry is  $-1$ . Angles are with respect to the direction specified by VEC. The SPn entries give the fractional solid angle  $f\text{sa}_i = [(1 - \mu_{i-1}) - (1 - \mu_i)]/2$  for the bin from  $\mu_{i-1}$  to  $\mu_i$ , and the SBn entries give the desired (biased) relative probabilities for emission in each angular bin. Note the first probability must be 0 for the unrealistic bin from  $(-\infty, -1)$ . From the true bin probabilities (from the SPn card), the weights of the source particles are adjusted by MCNP to remove the bias when scoring (or tallying) a history. A side note: it is not necessary to normalize the sum of the  $p_i$ s on the SPn or SBn cards. MCNP automatically ensures the probabilities are properly normalized.

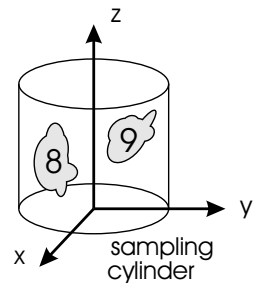
### 3.5.5 Multiple Volumetric Sources

#### Two Cylindrical Volumetric Sources

```

c --- Two volumetric sources uniformly distributed in cells 8 & 9.
c Both sources emit 1.25 MeV photons. Surround both source cells
c by a large sampling cylinder defined by the POS RAD and EXT
c parameters. The rejection technique is used to pick source
c points with cells 8 and 9 with the specified frequency.
c
SDEF ERG=1.25 CEL d1 AXS=0 0 1 POS 0 0 0 RAD d2 EXT d5
SI1 L 8 9 $ source cells: src 1 =cell 8, src 2 =cell 9
SP1 0.8 0.2 $ 80% from src 1; 20% from src 2
SI2 0 50 $ radius of cyl. containing cells 8 & 9
SI5 -30 30 $ axial range of cyl. containing src cells

```

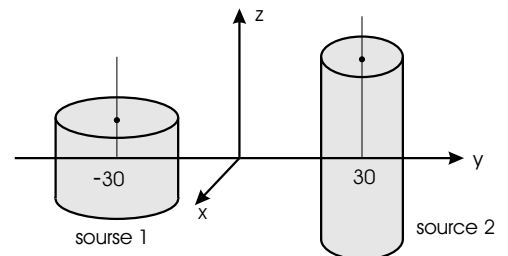


#### Two Cylindrical Sources with Different Energy Photons

```

c --- Two spatially different cylindrical monoenergetic sources.
c The size and position of each cyl. source depends on the
c source energy (FERG).
c
SDEF ERG=d1 POS=FERG d8 AXS=0 0 1 RAD=FERG d2 EXT=FERG d5
c
c -- set source energies: .667 MeV for region 1 and 1.25 MeV for region 2
SI1 L 0.667 1.25 $ fix energies: .667 MeV for region 1 and 1.25 MeV for region 2
SP1 0.4 0.6 $ 20% from src 1(Cs-137); 80% from src 2 (Co-60)
c -- set positions of the 2 source cylinders
DS8 S 9 10 $ get position for chosen source
SI9 L -30 0 0 $ center for sampling of src 1
SP9 1 $ prob. distn for src 1 center
SI10 L 30 0 0 $ center for sampling of src 2
SP10 1 $ prob. distn for src 2 center
c -- set radius and axial limits for each source
DS2 S 3 4 $ sampling distns from each src axis
SI3 0 20 $ radial sampling limits for src1
SP3 -21 1 $ radial sampling weight for src1 r^1
SI4 0 10 $ radial sampling limits for src2
SP4 -21 1 $ radial sampling weight for src2 r^1
DS5 S 6 7 $ axial sampling distns for each src
SI6 -10 10 $ axial sampling limits for src1
SP6 -21 0 $ axial sampling weight for src1 r^0
SI7 -30 30 $ axial sampling limits for src2
SP7 -21 0 $ axial sampling weight for src2 r^0

```

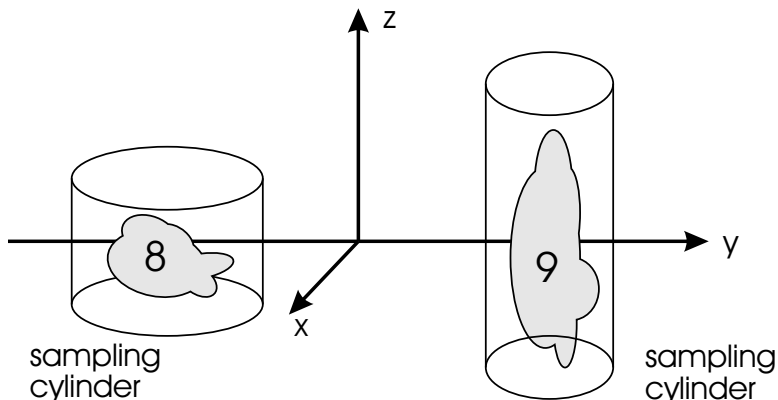


## Two Arbitrary Volumetric Sources with Different Energy Photons

```

c --- Two volumetric monoenergetic sources in complex-shaped cells 8 & 9
c   Spatial sampling uses the rejection technique by placing a finite
c   cylinder over each source cell. A random point inside a cylinder
c   is accepted as a source point only if it is inside the source
c   cell. Location and size of the sampling cylinders and source
c   photon energies are functions of the source cells (FCEL).
c
SDEF CEL=d1 POS=FCEL d2  AXS=0 0 1  RAD=FCEL d5  EXT=FCEL d8  ERG=FCEL d20
c
SI1 L 8 9          $ choose which cell source region to use for source
SP1  0.4 0.6      $ 40% from src 1; 60% from src 2
c -- set POS for each source
DS2 S 3 4          $ based on the cell chosen, set distribution for POS
SI3 L -30 0 0      $ center for spatially sampling of source 1
SP3  1            $ prob. distn for src 1 center
SI4 L 30 0 0       $ center for spatially sampling of source 2
SP4  1            $ prob. distn for src 2 center
c -- set RAD for each source (must completely include cells 8 or 9)
DS5 S 6 7          $ distns for sampling radially from each src axis
SI6  0 20         $ radial sampling limits for src1
SP6 -21 1         $ radial sampling weight for src1
SI7  0 10         $ radial sampling limits for src2
SP7 -21 1         $ radial sampling weight for src2
c -- set EXT for each source (must completely include cells 8 or 9)
DS8 S 9 10         $ distns for sampling axially for each src
SI9  -10 10       $ axial sampling limits for src1
SP9 -21 0         $ axial sampling weight for src1
SI10 -30 30       $ axial sampling limits for src2
SP10 -21 0        $ axial sampling weight for src2
c -- set energies of photons for each source
DS20 S 21 22
SI21 L 0.6938 1.1732 1.3325 $ Co-60 spectra for src 1
SP21 D 1.6312E-4 1 1        $ frequencies of gammas
SI22 L 0.667              $ Cs-137 spectrum for src 2
SP22 D 1

```



### 3.6 Tally Specifications

The tally command **F** tells MCNP what information about the radiation field should be calculated and output. MCNP6 has 12 basic tallies, which together with 20 ancillary commands and several variations of the basic tallies, allow the user to estimate a great many properties of the radiation field, such as doses at important locations from both primary and secondary particles.

With such flexibility afforded by the tally and associated commands, the about 10% of the *Manual* is devoted to this topic. The theory supporting the various types of tallies available in MCNP6 is given in Sections 2.5.1 to 2.5.9. The detailed description on the use of the tally and associated commands is in Sections 5.9.1 to 5.9.20. Finally many examples are provided in Section 10.2. A summary of available tallies in MCNP6 is given below.

**Table 5.** Types of tallies available in MCNP. The type of particle tallied is denoted by *pl*.

Mnemonic	Tally Type	F <sub>n</sub> Units	*F <sub>n</sub> Units
F1: <i>pl</i>	Integrated current over a surface	#	MeV
F2: <i>pl</i>	Average surface flux	# cm <sup>-2</sup>	MeV cm <sup>-2</sup>
F4: <i>pl</i>	Average flux in a cell(s)	# cm <sup>-2</sup>	MeV cm <sup>-2</sup>
F5a: <i>pl</i>	Flux at a point or averaged on a ring	# cm <sup>-2</sup>	MeV cm <sup>-2</sup>
FIP5: <i>pl</i>	pin-hole flux image	# cm <sup>-2</sup>	MeV cm <sup>-2</sup>
FIR5: <i>pl</i>	planar radiograph flux image	# cm <sup>-2</sup>	MeV cm <sup>-2</sup>
FIC5: <i>pl</i>	cylindrical radiograph flux image	# cm <sup>-2</sup>	MeV cm <sup>-2</sup>
F6: <i>pl</i>	energy deposition averaged over a cell	MeV g <sup>-1</sup>	jerks g <sup>-1</sup>
+F6	collision heating	MeV g <sup>-1</sup>	N/A
F7: <i>pl</i>	fission energy deposition in a cell	MeV g <sup>-1</sup>	jerks g <sup>-1</sup>
F8: <i>pl</i>	energy distn of pulses created in a cell	pulses	MeV
+F8: <i>pl</i>	charge deposition in a cell	charge	N/A

Tallies are identified by a unique tally id integer  $m < 10^8$ , the last digit of which specifies the tally type. Thus F4:P, F134:P, and F748374:P are all tallies for the average photon flux in a cell(s). Multiple F cards may be placed in Block 3. Thus, for example, one could use F2:N, F12:P, and F22:E to give the average surface flux of neutrons, photons, and electrons, respectively. Some tally types allow multiple types of particles. For example, an energy deposition tally for both gamma rays and electrons may be specified as F6:n,p. In the case of collision heating, +F6 always applies to all particles in a problem; therefore, this tally has no particle designator.

§5.9.1

The most frequently used tallies for fixed source problems are current at a surface (F1), average flux at a surface (F2), at a point or ring (F5), and flux averaged over a cell (F4). Similar to flux tallies over a cell are various tallies of energy deposition (F6 and F7). Unless otherwise specified with an FM card, tallies are normalized to one source particle. Except for tallies F6 and F7, designating a tally as \*F1:P, for example, multiplies the tally of each event by the photon energy. This results in tallies of energy flux or energy current. Tallies F6 and F7 are already in energy units.

The following sections describe the physical nature of several tallies. In the description, time dependence is suppressed, which is the normal case in MCNP calculations. The flux is integrated over time, and might better be called the fluence.

#### 3.6.1 The Surface Current Tally (Type F1)

Each time a particle crosses the specified surface, its weight is added to the tally, and the sum of the weights is reported as the F1 tally in the MCNP output. Note that there is no division by surface area  $A$ . Nor is there a distinction between direction of surface crossing. When used

§2.5.1

with problem geometry voided (zero density), the tally is useful for verifying conservation of energy and conservation of number of particles. Technically, if  $\mathbf{J}(\mathbf{r}, E, \Omega) \equiv \Omega \Phi(\mathbf{r}, E, \Omega)$  were the energy and angular distribution of the flow (current vector) as a function of position, the F1 tallies would measure

$$\begin{aligned} \text{F1} &= \int_A dA \int_E dE \int_{4\pi} d\Omega \mathbf{n} \cdot \mathbf{J}(\mathbf{r}_s, E, \Omega) \\ * \text{F1} &= \int_A dA \int_E dE \int_{4\pi} d\Omega E \mathbf{n} \cdot \mathbf{J}(\mathbf{r}_s, E, \Omega) \end{aligned}$$

where  $\mathbf{n}$  is the outward normal to the surface at  $\mathbf{r}_s$ .

### 3.6.2 The Average Surface Flux Tally (Type F2)

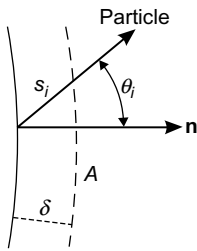


**Figure 4.** Particle crossing a surface at an angle  $\theta_i$  from the outward normal  $\mathbf{n}$ .

Often the fluence, averaged over some surface (or portion of a surface) is sought. Imagine a parallel surface a very small distance  $\delta$  from the surface of interest as shown in Fig. 4. The fluence (flux density integrated over all time or all simulated histories) is just the weighted sum of the path lengths of all the particles passing through this incremental volume  $\Delta V = A\delta$  divided by the volume of the extended region, i.e.,  $\Phi = \sum_i W_i s_i / \Delta V$ , where  $W_i$  is the weight of particle  $i$ . The path length for the particle shown is  $s_i = \delta / |\cos \theta_i|$  where  $\theta_i$  is the angle between the particle's exit direction and the outward normal  $\mathbf{n}$ . Thus, the fluence contribution of the  $i$ th particle crossing the surface is  $\Phi_i = \lim_{\delta \rightarrow 0} (W_i \delta / |\cos \theta_i|) / A\delta = W_i / (A |\cos \theta_i|) = W_i / (A |\Omega_i \cdot \mathbf{n}|)$ . Every time a particle crosses the surface, the value of its  $W_i / \cos \theta_i$  is added to the tally. Of course, many histories may not cross the surface in question and so no score is contributed to the tally. Finally, after  $N$  histories the average fluence, *per source particle*, is estimated as

$$\begin{aligned} \text{F2} &= \frac{1}{A} \int_A dA \int_0^\infty dE \int_{4\pi} d\Omega \Phi(\mathbf{r}, E, \Omega) \simeq \frac{1}{NA} \sum_{i=1}^N \sum_{j=1}^{n_i} \frac{W_i^j}{|\cos \theta_i^j|} \\ * \text{F2} &= \frac{1}{A} \int_A dA \int_0^\infty dE \int_{4\pi} d\Omega E \Phi(\mathbf{r}, E, \Omega) \simeq \frac{1}{NA} \sum_{i=1}^N \sum_{j=1}^{n_i} \frac{E_i W_i^j}{|\cos \theta_i^j|} \end{aligned} \quad (1)$$

where  $n_i$  is the number of surface crossing made by the  $i$ th particle,<sup>8</sup>  $W_i^j$  the  $i$ th particle's weight on its  $j$ th crossing, and  $\theta_i^j$  is the angle with respect to the outward normal at the  $j$ th crossing. Here  $\Phi(\mathbf{r}, E, \Omega)$  is the energy and angular fluence normalized to one source particle.

It should be noted that the variance of this fluence estimator is infinite and, hence, the central limit theorem can not be used to estimate confidence intervals. If many particles cross the surface in nearly tangential directions, i.e.,  $\cos \theta$  is very small, the tally contributions becomes very large. To avoid such large scoring events, MCNP sets  $|\mu| = 0.0005$  whenever  $|\mu| < 0.001$ . Because of this approximation the F2 surface flux tally is not quite exact.

### 3.6.3 The Average Cell Flux Tally (Type F4)

The idea behind the F2 tally, i.e.,  $\Phi = \text{sum of path lengths in } V/V$ , can also be extended to determine the average fluence in the volume of a cell. In this type of tally, the sum of path lengths  $s_i$  each particle makes in the volume  $V$  of interest is accumulated (see Fig. 5). Again, if a particle history never reaches the cell in question, then  $s_i = 0$ . The average fluence, per source particle, is then estimated as

$$\text{F4} \simeq \frac{1}{NV} \sum_{i=1}^N \sum_{j=1}^{n_i} W_i^j s_i^j,$$

<sup>8</sup>Typically  $n_i$  is 0 or 1. But a particle may make several crossing especially if the surface is re-entrant.



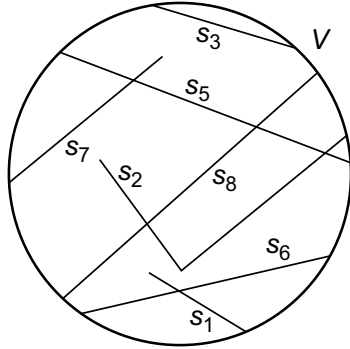


**Figure 5.** Particle paths in a cell of volume  $V$ .

particular, if  $\mathcal{R}(E) = 1$  or  $E$  one obtains **F4** or **\*F4**, respectively.

If the volume  $V$  is large so that many histories enter it, the path-length estimator is generally a good tally. If the region is a thin curved shell most track lengths have similar lengths and the estimator has a small variance. By contrast, for a regions bounded by two closely spaced parallel planes, there may be a wide variation in the track lengths through the region, and the resulting path-length estimator may have a large variance. The path length estimator is also computationally quite efficient, since particle tracking already computed the track lengths in the regions, so little extra effort is needed for this tally.

### 3.6.4 Flux Tally at a Point or Ring Detector (Type F5)

**Point Detector** A very powerful technique for scoring is to combine deterministic tally contributions and the stochastic collisions that occur during a history. One such estimator is the *next event estimator*. To simplify description of this type of tally, assume that calculations are being performed in a uniform medium. Consider the small spherical detector, with cross sectional area  $dA$ , shown in Fig. 6. A particle traveling in direction  $\Omega'$  has a collision at  $\mathbf{r}'$ . The collision may not be a scatter, and even if it were a scatter, it is very unlikely to scatter in the direction of the detector or even reach it to contribute to the fluence tally for the detector. However, one can analytically calculate the probability the particle will scatter at  $\mathbf{r}'$  and reach the detector without further interaction, and thus provide a contribution to the fluence tally for the detector, thereby short-cutting the Monte Carlo process.

§2.5.6.1

The probability the particle with energy  $E$  scatters at  $\mathbf{r}'$  through a scattering angle  $\theta_s$  and has a new direction of travel in  $d\Omega$  about  $\Omega$  with energy  $E'$  is<sup>9</sup>

$$p_1 = \frac{\mu_s(E, \omega_s) d\Omega}{\int_0^{2\pi} d\psi \int_{-1}^1 d\omega_s \mu_s(E, \omega_s)} = \frac{1}{2\pi} \left[ \frac{\mu_s(E, \omega_s)}{\int_{-1}^1 d\omega_s \mu_s(E, \omega_s)} \right] d\Omega = \frac{p(\omega_s)}{2\pi} d\Omega,$$

where  $p(\omega_s)$  is the PDF (defined by the terms in the square brackets) for scattering through an angle  $\theta_s = \cos^{-1} \Omega \cdot \Omega'$ . The distance between  $\mathbf{r}'$  and  $\mathbf{r}_d$  is  $R = |\mathbf{r}' - \mathbf{r}_d|$  so that  $d\Omega = dA/R^2$ . The probability that such a scattered particle actually reaches the detector without further collision is  $p_2 = \exp[-\mu_t(E')R]$ , where the argument of the exponential is the total number of mean-free-path lengths between  $\mathbf{r}'$  and  $\mathbf{r}_d$ .

The flux density can be interpreted as the number of particles entering a spherical detector of cross sectional area  $dA$  divided by  $dA$  [Shultis and Faw, 2002]. Thus, the contribution to the fluence made by the particle with weight  $W$  that interacts at  $\mathbf{r}'$  is

$$\delta\Phi = W \frac{\mu_s(E)}{\mu_t(E)} \frac{p_1 p_2}{dA} = W \frac{\mu_s(E)}{\mu_t(E)} \frac{p(\omega_s)}{2\pi R^2} \exp[-\mu_t(E')].$$

<sup>9</sup>Here  $\mu_i$  is the interaction coefficient or macroscopic cross section for interactions of type  $i$ . The *Manual* uses the symbol  $\Sigma_i$ .

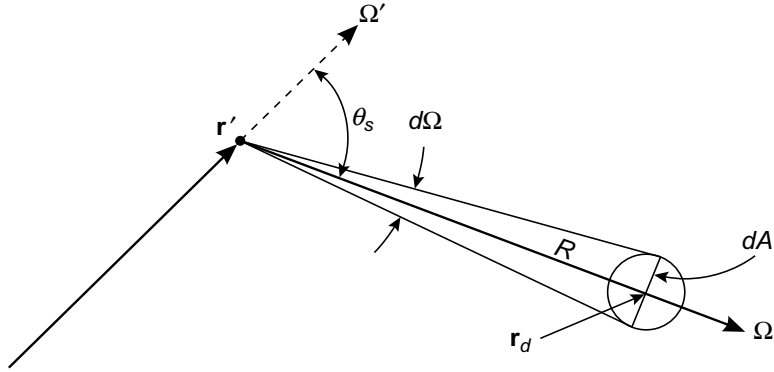


**Figure 6.** A particle moving in direction  $\Omega'$  makes a collision at  $\mathbf{r}'$  and scatters towards a small spherical detector at  $\mathbf{r}_d$  of cross sectional area  $dA$  and a distance  $R = |\mathbf{r}' - \mathbf{r}_d|$  from the scattering point.

This result is independent of  $dA$  and, thus, is used as a fluence tally for a point detector at  $\mathbf{r}_d$ . After each interaction in a particle's history, an estimate is made deterministically for the expected contribution of that interaction to the fluence at point  $\mathbf{r}_d$ .

A difficulty with this point detector tally occurs when the tally point lies within a scattering medium. Because of the  $1/R^2$  term in the above equation an enormous contribution is made to the tally if an interaction occurs very near the tally point. In fact, in a scattering region the variance of this estimator is infinite! An infinite variance, however, does not mean the tally cannot be used; indeed the tally will converge, but the asymptotic behavior is reduced to  $1/\sqrt[3]{N}$ , slower than the  $1/\sqrt{N}$  convergence for a tally with a finite variance [Kalos et al. 1968]. Of course, if the tally point is in a vacuum or non-scattering medium no such problem occurs.

MCNP avoids the infinite variance in a scattering medium by surrounding the tally point by a small sphere of radius  $R_o$  and, if an interaction occurs with  $R < R_o$ , the F5 tally records the average fluence uniformly distributed in the volume, i.e.,

$$\begin{aligned} \delta\Phi(R < R_o) &= \frac{\int \Phi dV}{\int dV} = W \frac{\mu_s(E)}{\mu_t(E)} \frac{p(\omega_s)}{2\pi} \frac{\int_0^{R_o} \frac{1}{r^2} e^{-\mu_t(E')r} (4\pi r^2) dr}{\frac{4}{3}\pi R_o^3} \\ &= W \frac{\mu_s(E)}{\mu_t(E)} p(\omega_s) \frac{3(1 - e^{-\mu_t(E')R_o})}{2\pi\mu_t(E')R_o^3}. \end{aligned}$$

Although the next event estimator can produce good estimates of the fluence at a point, its convergence may be rather slow. Further, F5 tallies are computationally expensive because a tally contribution is calculated every time a particle has any interaction even when it is far from the detector and makes very many small and negligible contributions  $\delta\Phi$ . This problem is aggravated with multiple F5 detectors.

§2.5.6.2 **Ring Detector** If the problem is axially symmetric about one of the coordinate axes, then a ring detector centered on the symmetry axis experiences the same fluence at all points on the ring. With a ring detector a point on the ring is randomly sample and the fluence contribution  $\delta\Phi$  is calculated as for a point detector for each interaction a particle makes. The advantage of a ring detector over a simple point detector is that sampling the tally point on the ring can be biased to obtain points closer to the interaction site, i.e.,  $R$  is smaller (and  $\delta\Phi$  larger) than if the sampling were uniform around the ring. The biased sampling is discussed in Section 2.5.6.2 of the *Manual*. Unlike the point detector, a ring detector has a finite variance.

### 3.6.5 Tally Specification Cards

At least one tally card is required, with the first entry on the card being  $Fn:pl$ , in which  $n$  is the tally id number (the last digit of which determines the type of tally), and  $pl$  stands for N (neutron tally), P (photon tally), N,P for joint neutron and photon tallies, and E for electron tallies. Following the tally type is a designation of the surfaces for the tally (types F1 and F2), or the cells (tally F4). For the type 5 detector tally, there follows a designation of the position of the detector. The energy deposition, pulse-height, and other specialized tallies are not discussed in this primer. In the subsections below, several examples are given to demonstrate the parameters on the  $Fn:pl$  card.

**Surface and Cell Tallies:** The card

§5.9.1.1

F1:E 1 2 T      \$ current through a surface

specifies electron current tallies through surfaces 1 and 2, and the total (T) over both surfaces. Note that the current tally is not divided by surface area. The card

F2:P 1 (1 2) (2 3 4) T      \$ fluence averaged over surfaces

specifies photon surface-integrated fluence tallies for surface 1, the average over surfaces 1 and 2, the average over surfaces 2 through 4, and the average (T) over all surfaces 1 through 4. Similarly, the card

F4:N 1 (2 3 4)      \$ fluences averaged over cells

specifies cell-averaged neutron fluence tallies for cell 1 and for cells 2 through 4. No composite average is called for.

**Point-Detector Tallies:** In the sense of an experiment or a Monte Carlo calculation, as the volume of a cell approaches zero, the path length segments in the cell and the number of particles intersecting the surface of the cell also approach zero and, hence, the flux tally becomes indeterminate. However, there is a way of computing the flux at a point by using the deterministic last-flight-estimator tally F5. This tally is invoked by a card such as

§5.9.1.2

F75:P X Y Z R      \$ point detector

Here 75 is the tally number, the last digit 5 denotes the F5 tally type, and P specifies the tally is for photons. The values of X, Y, and Z specify the coordinates of the point detector, and R designates the radius of a spherical exclusion zone surrounding the detector point. The need for an exclusion zone is evident from the  $1/r^2$  term in the flux contribution tallied, namely,

$$\delta\Phi = \frac{W}{4\pi r^2} e^{-\mu(E)r},$$

where  $r$  is the distance between the particle interaction site and the point detector. If  $r$  approaches zero, the tally contribution approaches infinity. Such large contributions make the F5 tally much less stable than the cell (F4) or surface (F2) flux tally. This instability is minimized by establishing a spherical “exclusion volume” of radius R centered on the point detector. For interactions occurring within this exclusion zone, an abnormally large tally contribution is avoided by scoring the fluence uniformly averaged over the exclusion spherical surface. The exclusion radius R can be specified, as a positive number (centimeters, and is the preferred method), or a negative number (mean free paths). Typically, R should be about 0.2 to 0.5 mean free path (averaged over the energy spectrum at the sphere). For a point detector inside a void region, no interactions can occur near the detector and R should be set to zero. Finally, several point detectors may be specified on one tally card, e.g.,

F5:P X1 Y1 Z1 R1 X2 Y2 Z2 R2

**Ring Detectors:** The manual also describes the use of a ring detector – useful for problems with symmetry about one of the problem axes. The form of this command is

§5.9.1.2.2

$Fna:pl a_o r \pm R_o$       \$ ring detector

where  $n$  is the tally number (last digit 5),  $a$  is X, Y, or Z to denote the symmetry axis,  $pl$  the particle type (P,N,...),  $a_o$  distance along axis  $a$  where the plane of the ring intersects the axis,  $r$  is the ring radius, and  $R_o$  is the exclusion radius around the ring (as discussed above).

§5.9.2 to  
§5.9.20

### 3.6.6 Cards for a Few Optional Tally Features

The MCNP6 *Manual* describes 20 optional commands that modify the output from a specified type of tally. Three such tally modification commands, which are frequently used, are sorting a tally into energy bins (the **En** card), multiply a tally by some quantity (the **FMn** card), and multiply each tally contribution by a fluence-to-response conversion factor (the **DEn** and **DFn** cards). These are addressed individually below.

§5.9.3

**The Tally Energy Card:** Suppose one wanted to divide the total flux or current normally produced by tally **Fn** into energy groups, say **E1** to **E2**, **E2** to **E3**, and **E3** to **E4**. This might be useful, for example, to isolate an uncollided component of the flux. This may be accomplished by use of a tally energy card (**En** card), such as

```
E24 E1 E2 E3 E4 $ energy bin boundaries
```

With this card the results for tally 24 (of type **F4**) are binned into four energy groups where **E1**, **E2**, **E3** and **E4** are the group (bin) upper limits. The lowest bin would extend down from **E1** to zero (or to a specified *cutoff energy*) for the type of particle being tallied. To create *m* equispaced bins between **E1** and **E<sub>max</sub>** use

```
E34 E1 mi Emax $ m linear interpolates + one bin from 0 to E1
```

If all tallies in a problem have the same energy group structure, a single card may be used, with **En** replaced by **E0**.

§5.9.9

**The Energy Multiplier Card:** Associated with the tally energy card is an optional energy multiplier **EMn** card of the form

```
EMn M1 M2 M3 M4 $ multiply energy bin k by Mk
```

Here the multiplier **M<sub>k</sub>** is applied to each contribution to the tally for the *k*th energy group. This card is useful, for example, to convert a fluence per source photon to a flux per curie source strength. For this example, one would add the following **EM** card for, say tally **F64**.

```
EM64 3.7E+10 $ (photons per sec)/curie (assuming 1 photon/decay)
```

The units of tally **F64** would then be “photons (cm<sup>-2</sup> s<sup>-1</sup>) per Ci.”

§5.9.8

**Dose Energy and Function Cards:** Suppose one wanted to compute a dose rate of some type associated with a flux or current tally, either total or by energy group. For example, suppose one wanted to compute

$$*F4 = \frac{1}{V} \int_V dV \int_E dE \int_{4\pi} d\Omega \mathfrak{R}(E) \Phi(\mathbf{r}, E, \Omega),$$

in which  $\mathfrak{R}(E)$  is a fluence-to-dose conversion factor. MCNP will carry out this calculation, obtaining values of  $\mathfrak{R}(E)$  by interpolation of values specified in a table placed in the input file. The form of the table is

```
DE4 A E1 E2 ... Ek $ energy grid for fluence-to-dose factors
DF4 B F1 F2 ... Fk $ fluence-to-dose conversion factors
```

Entries **E1** through **E<sub>k</sub>** are tabulated values of energy and **F1** through **F<sub>k</sub>** are corresponding tabulated values of  $\mathfrak{R}(E)$ . Entries **A** and **B**, either **LOG** or **LIN**, specify linear or logarithmic interpolation. If omitted, the default is logarithmic interpolation for both variables. If all tallies are to have the same dose conversion factors, a single table, designated by **DE0** and **DF0**, may be used to avoid repeating the table.

§6.9.2

**The Tally Comment Card:** If tallies are modified, it is good practice to explain the modification in a comment card that will be printed in the output file for the calculation. For example, an explanation of tally **Fn** could be entered in the card

```
FCn This tally has units of Sieverts per source photon
```

Continuation lines may be added so long as there are blanks in columns 1 through 5.

### 3.6.7 Miscellaneous Block 3 Commands

**The Mode Card:** This card is used to specify the type of particles to be tracked. Every input file must have a MODE card somewhere in block 3 of the input file. In the command line MODE *x*, the variable *x* may be just a single particle such as P, E, etc. or a combination such as N P E. A minus sign [-] in front of a particle's symbol means the antiparticle. Thus MODE E F, MODE E -E, and MODE F -F are equivalent. §5.7.1

**Time and History Cards:** The usual method for limiting how long MCNP runs is to specify either the maximum number of source particle histories or the maximum execution time. The maximum number of histories *N* is specified as NPS *N*. Alternatively, the maximum computing time *T*, in minutes, may be specified by the card CTME *T*. §5.13

**The Print-and-Dump Cycle Card:** By default, an output file is created only at the conclusion of a calculation, a binary continuation file, RUNTPE, is written every 15 minutes, and no tally-plot file, MCTAL, is written. Options to control the dump cycle are provided by the PRDMP card §5.13.5

```
PRDMP NDP NDM MCT NDMP DMMP
```

Here NDP is the increment for printing tallies in the output file (> 0 the number of histories, < 0 the time in minutes, = 0 for no intermediate dump); NDM is the increment for writing a continuation RUNTPE file (> 0 the number of histories, < 0 the time in minutes, = 0 to suppress all intermediate dumps); MCT is a flag to write tallies for plotting (1 yes, 0 no); NDMP is the maximum number of dumps written in the RUNTPE file (all by default); and DMMP is related to the use of multiple processors in the execution of MCNP. A typical card might read

```
PRDMP 0 -60 $ create continuation RNTPE every 60 min.
```

With this card, at most, 60 minutes of computing time would be lost if a calculation were aborted.

### 3.6.8 Short Cuts for Data Entry

*nR* repeats the preceding entry *n* times. Thus IMP:n 2 4R produces IMP:n 2 2 2 2.  
*nI* generated *n* linear interpolates. Thus E24 1 3I 5 produces E24 1 2 3 4 5.  
*xM* multiplies previous entry by *x*. Thus IMP:n 2 2X 3X 2X produces IMP:n 2 4 12 24.  
*nJ* jumps over *n* items. Thus PHYS:P 4J 1 changes the default physics PHYS:p 100 0 0 0 0 J 0  
PHYS:p 100 0 0 0 1 J 0.

## 3.7 Running MCNP6

§3.3.2

If the input file is named *inp*, then running MCNP is as simple as entering the the command MCNP6 in the MCNP command (DOS) window, which the installation of MCNP placed on your computer's desktop (after the window is set to the directory containing *inp*). However, one generally also specifies additional information. The general form of the executable command is

```
mcnp6 KEYWORD=value ... KEYWORD=value execution_option(s) other_options
```

where each instance of KEYWORD is one of 25 MCNP6 default file names (see Table 3.4 of the *Manual*) that the user wants to change, *execution\_option(s)* specify which of 5 execution module(s) are to be run, and *other\_option(s)* provides the user with additional execution control. The KEYNAME requires only enough letters of the default name to identify it uniquely. Much of this file renaming and option specification can be placed in block 0 (message block) of the input file to minimize typing for the MCNP6 executable command.

**Interrupting a Run:** MCNP6 allows the following interactive interrupts while running.

```
<ctrl+c>, k kills the job immediately without normal termination. If this re-  
quest fails, enter <ctrl+c> three or more times.  
<ctrl+c>, q stops the job normally after the current history  
<ctrl+c>, s gives the status of the job (number of particles and collisions pro-  
cessed so far and the time used)
```

## 4 Variance Reduction

§2.7

The challenge in using MCNP is to minimize the computing expense needed to obtain a tally estimate with acceptable relative error (as well as satisfying nine other statistical criteria). For many deep-penetration problems, a direct simulation (analog MCNP) would require far too many histories to achieve acceptable results with the computer time available. For such cases, the analyst must employ “tricks” to reduce the relative error of a tally (or its variance) for a fixed computing time, or to reduce the computing time to achieve the same relative error.

Two basic approaches can be applied to reduce the computational effort for a particular problem: (1) simplify the MCNP model, and (2) use non-analog simulations. In the first approach, the model geometry and the physics used to simulate particle transport can often be simplified or *truncated*. For example, it is a waste of computing effort to use a detailed geometric model of a region that is far from the detector tally location and that has little influence on the radiation field near the detector. Similarly, it is a waste of computer time to track neutrons as they thermalize in a shield if only the fast neutron fluence in some structural component is sought. For such a problem, once a neutron leaves the fast energy region, it can be killed without affecting the tally.

The second basic approach to reduce the variance of a tally is to modify the simulation process itself by making certain events more or less probable than actually occur in nature. Such a modified simulation is referred to as *nonanalog* Monte Carlo. As discussed in this section, MCNP has many nonanalog options many of which an analyst can use in combination to make a difficult analog problem much more tractable. These nonanalog tricks can be categorized into three general methods: (1) population control, (2) modified sampling, and (3) partially-deterministic calculations. In population control, for example, the number of particles in regions of high/low importance can be artificially increased/reduced. In modified sampling methods, certain events can be altered from their natural frequencies. Finally, in the partially-deterministic methods, part of the random-walk simulation can be replaced by a deterministic point-kernel type of calculation.

### 4.1 Tally Variance

§2.6.1

Before discussing the tricks used to reduce the variance of MCNP tallies, it is appropriate to examine exactly what it is that we are trying to reduce. When we run a Monte Carlo simulation, the  $i$ th history contributes a score  $x_i$  to the tally. If the particle (or its daughters) never reaches the tally region, then  $x_i = 0$ , whereas, if it reaches the tally without interaction, the score  $x_i$  often is very large. The probability any history will contribute a score between  $x$  and  $x + dx$  is denoted by  $p(x) dx$  where  $p(x)$  is a probability distribution function (PDF). In an MCNP simulation, we seek the mean score (or expected value) of  $x$ , namely

$$\langle x \rangle \equiv \int_0^{\infty} x p(x) dx. \quad (3)$$

Unfortunately, we don't know  $p(x)$  *a priori* (although MCNP will construct it and generate a plot of it — see Section 2.6.8.6). Instead, MCNP approximates  $\langle x \rangle$  by the average  $\bar{x}$  of the scores of  $N$  particles, i.e.,

$$\bar{x} \equiv \frac{1}{N} \sum_{i=1}^N x_i. \quad (4)$$

As  $N \rightarrow \infty$ , the *strong law of large numbers* guarantees that  $\bar{x} \rightarrow \langle x \rangle$ , provided  $\langle x \rangle$  is finite.

The variation in the different scores  $x_i$  is measured by the *standard deviation* of the population (histories), which for large  $N$

$$S^2 \equiv \frac{1}{N-1} \sum_{i=1}^N (x_i - \bar{x})^2 \simeq \overline{x^2} - \bar{x}^2, \quad (5)$$

where

$$\overline{x^2} \equiv \frac{1}{N} \sum_{i=1}^N x_i^2. \quad (6)$$

The estimated variance of the average  $\overline{x}$  is then

$$S_{\overline{x}}^2 = \frac{1}{N} S^2. \quad (7)$$

The *central limit theorem* states that if we repeated the simulation a large number of times (each with  $N$  histories), the variation of the means  $\overline{x}$  from each simulation will be distributed normally about the true mean  $\langle x \rangle$  and have a variance  $S_{\overline{x}}^2$ . It is this uncertainty or variance we are trying to reduce in our MCNP simulations, i.e., for a fixed number of particles, we seek an estimate  $\overline{x}$  which has the least uncertainty or minimum  $S_{\overline{x}}$ .

#### 4.1.1 Relative Error and FOM

In any variance reduction method, we change the simulation and hence change the underlying distribution  $p(x)$  so that it produces fewer zero-score histories and becomes more concentrated about its mean  $\langle x \rangle$ . By making  $p(x)$  more concentrated about its mean (which remains the same as the mean of the analog PDF), the variance of the mean  $S_{\overline{x}}^2$  will be less than that of the analog PDF, i.e., our estimate of the mean will be more precise.

§2.6.4

For each tally, MCNP not only calculates the sample mean  $\overline{x}$ , but several other statistics. One of the most important is the *relative error*  $R$  defined as

$$R \equiv S_{\overline{x}}/\overline{x}. \quad (8)$$

Clearly, we want to make  $R$  as small as possible with as few histories as possible. As discussed in the manual,  $R$  generally must be less than 0.1 for meaningful results (and even smaller if point/ring detectors are used). From Eqs. (7) and (8), it is seen that  $R \sim 1/\sqrt{N}$ . Thus increasing the number of particle histories is generally a very poor way of reducing  $R$ . This property of the relative error is the great weakness of the Monte Carlo method, because, generally, many histories must be generated to obtain acceptable results.

Another important statistic generated by MCNP is the *figure of merit* (FOM). This is defined as

§2.6.5

$$FOM \equiv \frac{1}{R^2 T}, \quad (9)$$

where  $T$  is the simulation time, which is proportional to  $N$  the number of histories run. Since  $R^2 \sim 1/N$ , we see that, except near the beginning of the simulation, the FOM should remain relatively constant. Also, for different simulations of the same problem, the simulation with the largest FOM is preferred since it requires the least time or produces a specified relative error.

Now on to ways of how to perform nonanalog techniques with MCNP.

## 4.2 Truncation Techniques

The basic idea behind truncation methods is to reduce the time per particle history by either simplifying the geometry or the physics used to generate the random walk for each particle. Proper application of this approach for variance reduction requires considerable experience and intuition by the analyst, since any simplification in the geometry or physics introduces a *bias* into the tally. Although a very *precise* (i.e., low variance or relative error) can be achieved, the tally estimate may not be very *accurate*. Generally, multiple runs with different approximations must be made to assess the importance of any simplification. MCNP can give you no warning about errors caused by geometric simplifications. Even for physics simplifications, MCNP produces, at best, a warning in the output, but no indication of whether serious bias has been introduced.

### 4.2.1 Energy, Time and Weight Cutoff

§5.7.4.1

The CUT command is used to specify a minimum energy, time, or particle weight below which the particle is killed. The values specified on the CUT card apply everywhere in the geometry. Here is an example:

```
CUT:p j 0.075 $ kill photons with E < 75 keV
```

In this example, whenever a photon falls below 75 keV, it is killed. The CUT command has 5 parameters. The first is a time limit for an individual history, which in the above example is specified as j to jump over the default value of a very large time. Parameters 3 to 5 are limits on the weights of particles.

§5.7.4.6

The ELPT is like the CUT card, but allows you to specify the cutoff on a cell-by-cell basis. For example,

```
ELPT:p 0.01 0.02 0.03 0.04 0.05 $ energy cutoffs
```

terminates photons in cell 1, 2, 3, 4, and 5 that have energies less than 10, 20, 30, 40, and 50 keV, respectively. Should both the ELPT and the global CUT commands be used, the higher limit prevails.

The CUT and ELPT commands are particularly useful for energy deposition tallies for which low energy particles make little contribution. However, for neutron problems, use CUT and ELPT carefully since low energy neutrons cause most of the fissions and produce most of the capture gamma photons.

### 4.2.2 Physics Simplification

§5.7.2

The PHYS command is used to specify energy cutoffs and the physics treatments to be used for photons, neutrons and electrons. Each particle has different parameters which are specified with this command.

**Photons:** There are two inherent physics approximations for photon interactions in MCNP: (1) only K and L edges are considered for photoelectric interaction, and (2) no triplet production (pair-production near an orbital electron). In addition, other physics simplifications can be imposed with the PHYS card. This card has the form

```
PHYS:P EMC PF IDES NOCOH PNINT NODOP
```

The EMC PF parameter is the energy in MeV above which simple physics is to be used. In simple physics, no fluorescence from photoelectric interactions is produced, no binding effects are used in photon scattering, and no coherent scattering is included. IDES= 0/1 indicates that Bremsstrahlung is included/ignored for MODE P and, for MODE P E, electron production and transport is used/not used. NOCOH= 0/1 specifies that coherent scattering is included/ignored. PNINT= -1/0/1 indicates photonuclear interactions are used in an analog manner / not used / used with a bias. If PNINT≠ 0 there must be a MPNn card following the material Mn card. Finally, NODOP= 0/1 turns Doppler broadening (from the speed of bound electrons) on/off. The default is

```
PHYS:P 100 0 0 0 0 $ 100 MeV, brems, coh scat, no photonuc, Doppler
```

The various physics options selected can greatly affect the run time, especially if electron transport is turn on. As an example of how different physics simplifications can affect the run time, consider a point isotropic source emitting 7-MeV photons into an infinite iron medium. The ambient dose equivalent 20 cm from the source is estimated by using an F2 spherical surface detector. In Table 6 the tally mean and the runtime are shown for different physics assumptions. Notice that turning Bremsstrahlung off more than halves the compute time with only about a 15% reduction in the estimated dose. Thus, the no Bremsstrahlung option is very effective for initial scoping calculations. Also notice that using simplified photon physics increases the compute time, a mystery to the authors. Although not shown in the table, if secondary electron transport had been used instead of the thick-target Bremsstrahlung approximation (by invoking the MODE P E command) the compute time is very much longer (about 1700 minutes for the test problem). Use electron transport only when necessary!



**Table 6.** MCNP6.2 results with different physics models for a point 10-MeV photon source in an infinite lead medium. Tally is the ICRP 1987 ambient dose equivalent at 5 cm from the source. Results are for simulations of  $4 \times 10^6$  source photons, split among 8 tasks, on an Apple M2 Pro Mac Mini All cases passed the 10 statistical tests, unless otherwise noted.

MCNP6 Commands	Description*	F2 Tally (Sv/photon)	Relative Error	FOM	mcrun Time (min)
PHYS:P 100.0 0 0 0 0 J 0	default: dphys + brem + coh + no pn + dop	1.20610E-14	0.0010	293 393	3.31
PHYS:P 10.0 0 0 0 1 J 0	dphys + brem + coh + no pn + no dop	1.20597E-14	0.0010	293 685	3.26
PHYS:P 10.0 0 1 0 1 J 0**	dphys + brem + no coh + no pn + no dop	1.20609E-14	0.0010	290 038	3.21
PHYS:P 0.0 0 0 0 0 J 0***	sphys + brem + coh + no pn + dop	1.20775E-14	0.0010	148 802	6.60
PHYS:P 0.1 0 1 0 1 J 0	sphys > 10 keV + brem + no coh + no pn + no dop	1.20873E-14	0.0010	145 006	6.73
PHYS:P 10.0 1 1 0 1 J 0	dphys + no brem + no coh + no pn + no dop	7.11461E-15	0.0015	864 296	0.49
PHYS:P 0 1 1 0 1	sphys + no brem + no coh + no pn + no dop	7.11551E-15	0.0015	965 105	0.44
no PHYS card CUT:p j 0.1**	default: + kill photons if $E < 0.1$ MeV	1.20321E-14	0.0010	696 922	1.32

\* dphys = detailed physics, sphys = simple physics; coh = coherent scatter; pn = photonuclear brem = Bremsstrahlung; dop = Doppler broadening

\*\* Did not pass VoV Decrease Rate Test

\*\*\* Did not pass PDF Slope Test

**Neutrons:** MCNP with its integrated neutron cross section libraries is an ideal tool for neutron transport studies. Nevertheless there are several approximations MCNP uses for neutron interactions: (1) secondary particles from neutron interactions are sampled independently, (2) delayed gammas from fission products are ignored so about one-half of the steady-state gamma-ray energy is ignored, (3) treatment of temperature effects with the  $S(\alpha, \beta)$  method is limited to about 15 moderators, and (4) the number of fission neutrons is always sampled from the closest two integers about  $\nu(E)$ .

For neutrons the PHYS card has only four parameters, namely

```
PHYS:N EMAX EMCNF IUNR DNB
```

The EMAX parameter is the energy in MeV above which neutron data is not placed in memory (default is very large). Neutrons below EMCNF (in MeV) are treated by analog capture while above EMCNF implicit capture is used (see next section). If IUNR= 1 the averaged cross sections above the resolved cross section region are used, while if IUNR= 0 (the default) probability tables, describing interactions over the myriad levels and widths of the unresolved resonances, are sampled. The final parameter DNB specifies if  $\nu(E)$  includes prompt plus delayed neutrons (= -1, the default), or if only prompt neutrons are included (= 0), or if DNB(> 0) delayed neutrons per fission are to be used. Here is an example.

```
PHYS:n 5.0 0.1 $ max sigma table energy; analog capture below 100 keV
```

Here cross section data only below 5 MeV is retained (to save data storage memory). For neutrons

below 0.1 MeV, analog absorption (direct simulation) will be used, while above 0.1 MeV, implicit absorption is used.

#### 4.2.3 Histories and Time Cutoffs

Normally an MCNP run is terminated when a certain number of particle histories have been run or a desired computing time has been exceeded. These cutoffs are specified by the NPS and CTME commands such as

```
NPS 1000000 $ stop after a million source particles have been run
CTME 20.0   $ stop run after twenty minutes
```

If both are specified, the first cutoff to occur causes program termination.

### 4.3 Nonanalog Simulation

In many problems, very few of the source particles reach the detector or region used for the tally, i.e., most particles produce a zero *score*. The number of particles reaching the tally region can, however, often be dramatically increased by abandoning a strict analog simulation. Of course, the expected value of the tally must not be changed. How can the tally remain unchanged when we artificially force more particles to the scoring region? The key is to assign each particle a *weight*, and, as the particle is “forced” towards the scoring region, the particle weight is decreased in a manner such that the average of the particle weights reaching the detector is the same as the expected tally in a true analog simulation. Thus, if we make a certain event in a particle history  $m$  times more likely, we must multiply the particle’s weight by  $1/m$  to avoid biasing the tally expectation.

MCNP has many nonanalog simulation options whose use, often in combination, can decrease the variance of a tally without increasing the computational expense.

#### 4.3.1 Simple Examples

To understand the basic idea of nonanalog techniques, consider the simple slab transmission problem illustrated in Fig. 7. In this problem a point isotropic source is placed on one side of a slab shield, and the problem is to determine the fraction of source particles that reach the opposite face of the slab. A direct analog simulation is represented by Fig. 7(a).

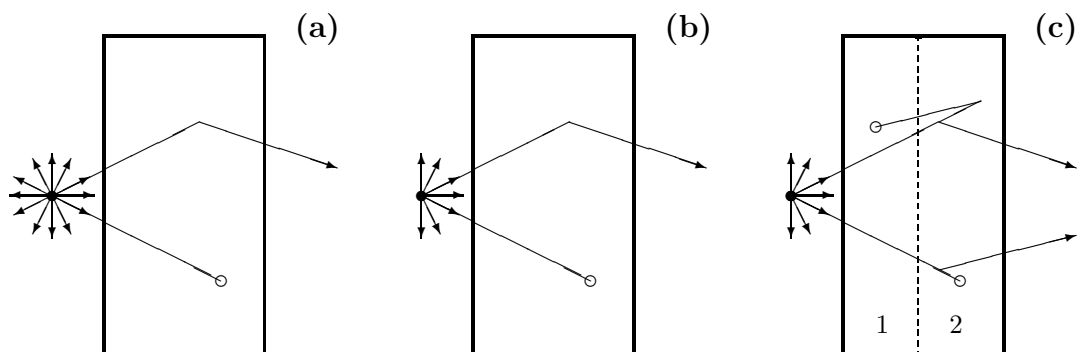


Figure 7. Examples of analogue and nonanalogue Monte Carlo simulations.

æ

**Source Biasing:** A non-analog simulation can considerably reduce the computing effort compared to an analog simulation. For example, in the analog simulation half of the source particles are

“wasted”, i.e., those emitted away from the slab cannot reach the scoring surface and computer time is wasted sampling backward source directions and tracking these particles to the left problem boundary. It would be more efficient to start each source particle towards the slab, as shown in Fig. 7(b). However, by restricting or biasing the source emission directions to only those oriented toward the slab, twice as many particles will subsequently penetrate the slab in case (b) compared to analog case (a), for the same number of particle histories tracked. To avoid doubling the transmission tally (no. transmitted per real (analog) source particle), we adjust the source particle’s weight in the biased simulation to be 0.5. Thus the average of the *weights* of transmitted particles still equals the particle transmission fraction obtained with the analog simulation. Moreover, for the same number of source particles, twice as many reach the tally surface in case (b) compared to case (a), and thus the variance of the case (b) tally is less.

**Splitting:** Another technique for increasing the number of particles reaching the scoring surface is illustrated in Fig. 7(c). Here the slab is conceptually divided into two sublayers. Whenever a particle crosses from the layer nearest the source to the layer nearest the tally surface, it is *split* into two particles, each with half of the original particle’s weight and both moving with the same velocity as the original particle. The random walk simulation is then performed independently for each new particle, beginning at the entry point into the second layer of the original particle. Twice as many particles will now reach the tally surface (thereby reducing the tally’s variance); but, since their weights have been reduced by one-half, the expected tally value remains unchanged.

**Russian Roulette:** When a particle reaches a region of space far from the tally region it is unlikely, with further random walk simulation, to reach the tally region, and the run time can be reduced by terminating or killing such a particle. Thus, in the example case (c), when a particle in the right-hand sublayer returns to the first left sublayer, we may think it has a relatively poor chance of returning yet again the right sublayer and reaching the tally surface. When a particle reenters the first layer from the second, the particle is hence killed with a probability of 0.5. If the particle survives this winnowing process, its weight is increased by a factor of two, to keep the simulation unbiased, and the particle’s random walk continues.

**Implicit Absorption:** Those particles which are tracked through the slab but are absorbed before they reach the tally surface represent wasted computing effort. Another variance reduction trick is to replace *analog capture* with *implicit capture*. At a collision site, a particle is killed, in an analog simulation, with a probability  $\sigma_a/\sigma_t$  (analog capture). However, in implicit capture, the particle is allowed to continue on its trajectory as if no interaction had occurred but with the particle’s weight changed to  $1 - (\sigma_a/\sigma_t)$  times its original weight. In this way, no particles are lost due to absorption, but absorption effects are properly accounted for.

## 4.4 MCNP Variance Reduction Techniques

MCNP offers a variety of variance reduction techniques based on different nonanalog simulations. The art of using MCNP to solve difficult problems is to use these program features to obtain both precise and computationally efficient results. In this section, the use of several of the most useful variance reduction techniques are described.

§2.7.2.1-4 ,  
§5.12

The variance reduction techniques offered by MCNP can be categorized as follows:

1. *Population Control Methods:* These methods artificially increase/decrease the number of particles in spatial or energy regions that are important/unimportant to the tally score. Specific population control methods include
  - Geometry splitting and Russian roulette (IMP)
  - Energy splitting/roulette (ESPLT)
  - Weight cutoff (CUT, PWT)

- Weight windows (WWE, WVN, WVP, WWG, WWGE)
2. *Modified Sampling Methods:* These methods artificially increase the likelihood of events that increase the probability a particle reaches the tally region. Included in MCNP are
    - Exponential transform (EXT, VECT)
    - Implicit capture (PHYS)
    - Forced collisions (FCL)
    - Bremsstrahlung biasing (BBREM)
    - source direction and energy biasing (SDEF, SP, SB, SI)
    - neutron-induced photon production biasing (PWT)
  3. *Partially Deterministic Methods:* These method replace the random-walk process by a deterministic process (e.g., exponential attenuation) to move particles from one region to another. In MCNP the following are available:
    - Point and ring detectors (F5a)
    - DXTRAN spheres (DXT, DXC)
    - Correlated sampling (PD)

The selection of effective variance reduction methods for a particular problem requires considerable experience and skill on the part of the analyst in interpreting the MCNP output. To gain experience in using these variance reduction techniques, the novice is encouraged to try using them on simple problems, sometimes separately and sometimes in various combinations. Through such experimentation, valuable experience and insight into variance reduction is gained. In the sections below, some of the simpler variance reduction techniques are discussed and illustrated.

#### 4.4.1 Geometry Splitting

In geometry splitting, *importances* are assigned to each cell in the problem. Generally, cells near the tally region should have a greater importance than cells farther away. When a particle leaves a cell with importance  $I_1$  and enters a cell of importance  $I_2$ , the particle is split/rouletted according to the ratio  $I_2/I_1$ . For example, if  $I_2/I_1 = 2.75$  the entering particle is split into three particles with 75% probability and into two particles with 25% probability. If  $I_2/I_1 = 0.6$ , the entering particle is killed with 40% probability and allowed to survive with 60% probability. Of course, in each splitting or Russian roulette the weight of the remaining particles is adjusted to leave the tally unbiased. This technique of geometry splitting with Russian roulette is very reliable since, if no other biasing techniques are used, all the particles in a cell will have the same weight regardless of the paths taken to reach the cell. The importance of a cell can be defined on the cell definition line, such as

```
c      Set cell importance on the cell definition line
20 1  -7.86  10 -20  IMP:p=7  $ cell 20; matl 1; density; defn; importance
```

or the importances of all cells can be set in Block 3 with the IMP command

```
c      Set cell importances in a geometric progression
IMP  1 2m 2m 2m 2m 2m 0  $ import. of cells 1--7 = 1 2 4 8 16 32 0
```

The importance of a cell is intimately related to the average adjoint fluence in the cell (a quantity generally not known *a priori*). As a practical matter, the cell importances should be adjusted so as to keep the population of particles in the cells relatively constant as one moves from the source region to the tally region. First, perform a short run with all importances set to unity, examine the “cell population” found in output print table 126, and estimate the cell importances by the ratio of cell populations  $P$  in adjacent cells, i.e.  $I_n \simeq P_{n-1}/P_n$ . Typically, source cells have an importance of unit and cells closer to the tally region have larger importances.

Adjacent cells should not have importances that are greatly different. As a rule, the ratio of importances in adjacent cells should not exceed a factor of 6 to 8. Consequently, it is often necessary to subdivide cells into many cells to prevent adjacent cell importances from changing too rapidly. It should also be remembered that, when Russian roulette is used to terminate some particles, information is lost; subsequent building up the particle population with large cell importances cannot regain this lost information.

A warning about large importances. In problems with large attenuation of particles between the source and tally region, importances of cells near the tally can reach many orders of magnitude. For these cases, if a VOID command is used to flood the geometry with particles in order to find geometry errors, the cell importances are still in effect, and a few source particles will be magnified into millions of particles, all of which MCNP must track. Instead of a short run, hours or days can be required!

#### 4.4.2 Weight Windows

The weight-window variance reduction technique adjusts the weights of particles as they change energy and move through the various cells in the problem geometry. In each cell, a lower weight bound and an upper bound (defined as a multiple of the lower bound) are specified. If a particle entering a cell or a particle created in the cell has a weight above the upper bound, the particle is split such that all split particles are within the weight window. Similarly, if a particle has a weight below the lower bound, Russian roulette is used to increase the particle's weight until it lies within the window or until it is killed. In most problems weight-windows is preferred over importance biasing.

§2.7.2.12 ,  
§5.12.3

##### Advantages:

- Weight-windows can equalized the weights of scoring particles, by requiring important regions to have small weight windows, thereby producing a tally with a small variance. (Recall if every particles gives the same score, an answer with zero variance is obtained.)
- The weight-windows variance reduction technique is a space and energy biasing scheme, whereas importance sampling is only a spatial biasing technique.
- Weight window discriminates on particle weight before taking appropriate action. Geometry splitting is done regardless of the particle's weight.
- Weight windows uses absolute bounds, whereas geometry splitting is based on ratios so that a particle's weight can grow or decrease without limit. This is particularly useful when using ring and point detectors with which large particle weights can cause large tally perturbations.
- Weight windows is applied at surfaces and collision sites whereas geometry splitting occurs only at surfaces.
- Weight windows is immune to weight fluctuations caused by other biasing techniques, whereas geometry splitting preserves such fluctuations.
- Weight windows can be turned off in large cells, in which no single importance applies, by setting the lower limit to zero.
- Weight windows can be generated automatically by MCNP whereas cell importances requires considerable insight by the user.
- Weight windows is more compatible with other variance reduction techniques such as the exponential transform.
- Weight Windows can be based on user-defined meshes superimposed on the geometry.

##### Disadvantages:

- Weight windows is not as straight forward as geometry splitting. Without the automatic weight-window generator, weight windows would be very difficult to use since window limits of each cell are difficult to predict. By contrast, cell importances are much easier to guess.

- When the weight of source particles is changed, the weight-window limits have to be renormalized.

#### §5.12.14.1

**Generating Weight Windows** The weight-windows biasing is specified with the `WWE`, `WWN`, and `WWP` commands. The reader is referred to the manual for the command parameters. However, the non-expert rarely enters these command directly; rather, the *weight-windows generator* is usually used to automatically calculate these commands and their parameters.

To use the weight-window generator, the `WWG` (and, optionally, the `WWGE`) commands are placed in Block 3 of the input file. The `WWG` command is

```
WWG It Ic Wg j j j j IE
```

where  $I_t$  is the tally number,  $I_c$  is a reference (usually source) cell,<sup>10</sup>  $W_g$  is the value of generated lower weight-window bound (if 0, set to 0.5 of source particle weight), the next four parameters are not used and simply “jumped” (j) over,<sup>11</sup> and  $I_E = 0$  specifies the generated `WWGE` card is for energy bins while  $I_E = 1$  means time bins are used.

The optional `WWGE` can be included generate weight windows for a set of contiguous energy bins. This command is

```
WWGE:n E1 E2...Ej
```

where  $n = N/P/E$  for neutrons/photons/electrons,  $E_i$  is the upper energy bound for weight-window group ( $E_{i+1} > E_i$ ), and  $j$  is the maximum number of energy groups ( $j \leq 15$ ).

As an example, for a point photon source in cell 10 and tally F2, the following weight-window generator command

```
WWG 2 10 0 j j j j 0 $ generate weight windows using energy bins
```

is placed in Block 3 of the input. Near the end of the resulting output file, lines similar to the following appear.

```
wwp:p 5 3 5 0 0 0
wwe:p 1.0000E+02
wwn1:p 5.0000E-01 5.0000E-01 4.0810E-01 2.5853E-01 1.5586E-01
      9.1319E-02 5.2707E-02 3.0064E-02 1.6959E-02 9.4621E-03
      5.2438E-03 2.8816E-03 0.0000E+00 -1.0000E+00
```

The ten leading blanks on these lines are edited out, the weights inspected and changed if necessary to ensure there are no spurious fluctuations (caused by incomplete sampling), and then these lines are placed in Block 3 of the input for a second run. This iteration process can be repeated to perfect the “best” weight windows.

### 4.4.3 An Example

Consider a point isotropic source emitting 7-MeV photons surrounded by an iron annular spherical shell 30-cm in thickness with an inner radius of 30 cm. The ambient dose 160 cm from the source is sought. Three approaches are used: (1) analog simulation, (2) geometry splitting, and (3) weight windows. The MCNP input file for the analog simulation is shown in Fig. 8.

With this thick iron shield, few source particles penetrate the shield, and hence we need to use some biasing technique to help particles through the shield. This problem is ideally suited for geometry splitting. To implement this, split the 30-cm spherical cell into 10 cells, each 3-cm in thickness. Examination of the output produced when this 10-cell shield problem is run as an analog simulation shows that the photon population in each shield cell decreases by about a factor of two

<sup>10</sup>If  $< 0$  weight windows is based on a user specified mesh, but we do not discuss this in this primer.

<sup>11</sup>These parameters were used in debugging the weight window algorithm.

```

Point isotropic 7-MeV photon sources in iron shell: (analog base case):
c ***** BLOCK 1: CELL CARDS *****
c GEOMETRY:      X isotropic point source (7-MeV)
c                D ambient dose 100 cm from outer shield surface (160 cm)
c                iron shield 30-cm thick (r=30 to 60 cm)
c                (without shield, dose is 6.013x10-17 Sv/gamma)
c
c
c                z-axis ^
c                |      \      \      \      void
c                |      \      \      \
c                | void |      \      \
c                |      |      \      \
c                X -----|-----D-----> x-axis
c                source  |      |
c                |      /      /      /
c                |      /      /      /
c
c ***** BLOCK 1: CELLS *****
10 0          -10          imp:p=1  $ inside of shield
20 1   -7.86   10 -20      imp:p=1  $ iron shell
30 0          20 -50      imp:p=1  $ void outside shld and inside detect
40 0          50 -100     imp:p=1  $ void past detector
50 0          100          imp:p=0   $ vacuum outside problem boundary

c ***** BLOCK 2: SURFACE CARDS *****
10 so 30.0          $ inner shield surface
20 so 60.0          $ outer shield surface
50 so 160.0         $ detector surface
100 so 10.E+02      $ spherical problem boundary (at 10 m)

c ***** BLOCK 3: DATA CARDS *****
SDEF erg=7.00 par=2      $ 7-Mev pt photon source at origin
c
mode p
phys:p 100 1 1        $ no bremsstrahlung; no coherent scattering
nps 10000             $ 10000 particle cutoff
f2:p 50               $ tally on surface 50 as ambient dose
c
c ---- Photon ambient dose equivalent H*(10mm) Sv cm2; ICRP [1987]
de2  0.100E-01 0.150E-01 0.200E-01 0.300E-01 0.400E-01 0.500E-01
      0.600E-01 0.800E-01 0.100E+00 0.150E+00 0.200E+00 0.300E+00
      0.400E+00 0.500E+00 0.600E+00 0.800E+00 0.100E+01 0.150E+01
      0.200E+01 0.300E+01 0.400E+01 0.500E+01 0.600E+01 0.800E+01
      0.100E+02
df2  0.769E-13 0.846E-12 0.101E-11 0.785E-12 0.614E-12 0.526E-12
      0.504E-12 0.532E-12 0.611E-12 0.890E-12 0.118E-11 0.181E-11
      0.238E-11 0.289E-11 0.338E-11 0.429E-11 0.511E-11 0.692E-11
      0.848E-11 0.111E-10 0.133E-10 0.154E-10 0.174E-10 0.212E-10
      0.252E-10
c
c --- Natural iron (density 7.86 g/cm3)
m1  26000 -1.00000

```

Figure 8. Input for analog simulation of example problem.

over its neighbor closer to the source. Thus, to use geometry splitting, change the importances of the shield cells to 1 for the innermost iron cell, 2 for the next, 4 for the next, and so on to the tenth cell with an importance of  $2^9 = 256$ . This is done with the IMP command

```
c Importances: 1 src cell; 10 shld cells; 2 outer cells; 1 boundary cell
IMP:p 1 1 2m 2m 2m 2m 2m 2m 2m 2m 2R 0 $ cell importances
```

The mean and relative error with such a nonanalog simulation are shown in Figs. 9 and 10. For this nonanalog simulation, the figure-of-merit (FOM) was 4.9 times larger than that for the analog simulation, so that, to achieve the same relative error, the analog simulation would have to be run  $4.9^2 = 24$  times longer.

An alternative approach is use weight windows for the 10-cell shield model. First run the problem as an analog problem with the weight window generator command placed in Block 3. Here we use

```
WWG 2 10 0 j j j j 0 $ ask WW generator to find weights
```

Then place the generated weight-window cards written near the bottom of the output (with the appropriate blanks removed) into Block 3 and rerun as a weight-window biased simulation. The results are also shown in Figs. 9 and 10. For this weight-window simulation, the figure-of-merit (FOM) was 5.4 times larger than that for the analog simulation.

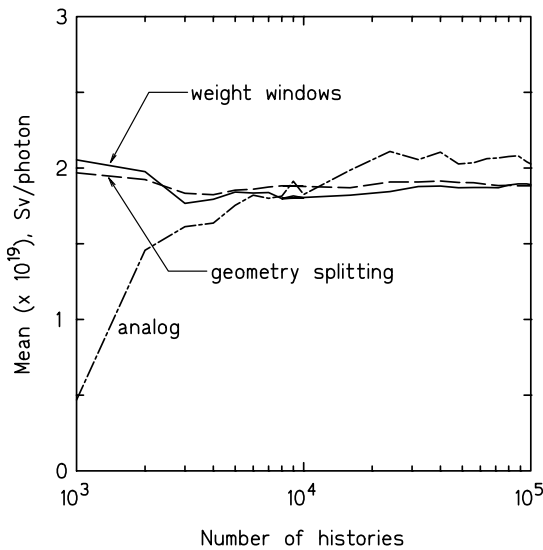


**Figure 9.** The mean of the tally for the example problem.

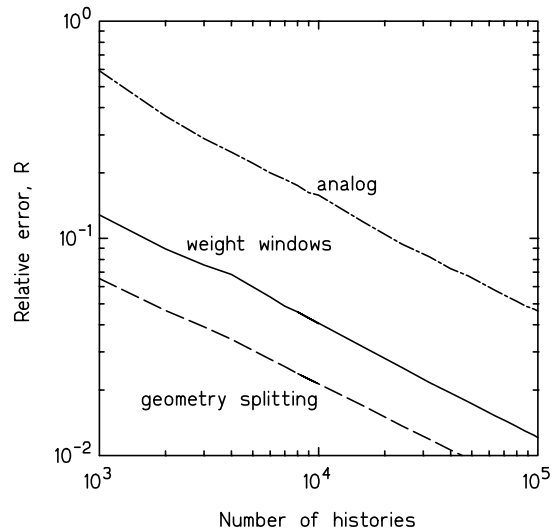


**Figure 10.** The relative (fractional) error for the test problem.

#### 4.4.4 Exponential Transform

§2.7.2.13 ,  
§5.12.7

The exponential transform artificially changes the distance to the next collision. In this technique, particles can be moved preferentially towards the tally region and inhibited from moving away from it. The exponential transform stretches the path length between collisions in a preferred direction by adjusting the total cross section as  $\Sigma_t(1 - p\mu)$  where  $p$  is the stretching parameter, and  $\mu$  is cosine of the angle between the particle direction and the preferred direction.

The exponential transform biasing is invoked with the EXT and VECT commands. The EXT command has the form

```
EXT:n A1 A2 ... Ai ... Aj
```

where  $n = N/P/E$  for neutrons/photons/electrons, and for the  $i$ -th cell  $A_i$  has the form  $Q V m$ , and  $j$  is the number of cells. Usually  $Q = p$ , while  $Q = 0$  indicates the exponential transform is not to



be used (and  $V$  and  $m$  are omitted). The stretching direction is specified by the  $V$  and  $m$  part of  $A_i$  and the VECT command.

#### 4.4.5 Energy Splitting/Russian Roulette

In some problems, e.g., finding the high-energy neutron fluence in a pressure vessel, only particles with a certain range of energies are of interest. When such a particle is created, the ESPLT command can be used to split the particle into more daughter particles of the same type. Also, when a particle of energy outside the energy region of interest is created, Russian roulette is used to eliminate some of these particles. An example of the ESPLT command is

§2.7.2.8 ,  
§5.12.5

```
c    Energy splitting with Russian roulette
c    split to 4 for 1 if parent energy falls below 3 MeV
c    split to 2 for 1 if parent energy falls below 1 MeV
c    split to 1 for 2 if parent energy falls below 0.4 MeV
c    split to 1 for 4 if parent energy falls below 0.1 MeV
ESPLT:n  4 3  2 1  0.5 0.4  0.25 0.1
```

#### 4.4.6 Forced Collisions

The forced collision biasing method increases the sampling of collisions in specified cells, generally those near a DXTRAN sphere or point/ring detector. This method splits particles into collided and uncollided parts. The collided part is forced to interact within the current cell while the uncollided particle exits the cell without collision. The weight windows game is not played at surfaces bounding a cell in which forced collisions are specified. The forced collision option is invoked with the command

§2.7.2.15 ,  
§5.12.9

```
FCL:n  x1 x2 ... xi ... xj
```

where  $n = N/P$  for neutrons/photons,  $j$  is the number of cells, and  $x_i$  controls which particles undergo forced collisions (see manual for details)

#### 4.4.7 Source Biasing

One of the easiest nonanalog techniques to implement is *source biasing*. In MCNP, any of the SDEF variables can be biased. For example, source particles can be started with enhanced weights, with preferred energies, and in regions closer to the detector. One of the most useful source biasing techniques is to start particles in preferred directions, generally towards tally regions.

§2.7.2.16 ,  
§5.8.4

As an example, consider the spherical iron shell problem of Section 4.4.3. Rather than use a spherical F2 detector at 160 cm from the source, place a point detector on the x-axis 160 cm from the point source. (This is a terrible idea compared to using the surface F2 detector, but it illustrates the importance of source biasing.) Then to start particles preferentially towards the detector on the positive x-axis, we might use

```
SDEF  ERG=7.00  PAR=2  VEC=1 0 0  DIR=d1  $ bias source direction
SB1   -31  2.0      $ exp bias exp[2mu]
```

Here source particles will be emitted with the PDF  $p(\mu) = Ce^{K\mu}$  where  $\mu = \cos\theta$ , the cosine of the angle between the emission direction and the VEC direction (here the x-axis).  $C$  is a normalization constant  $C = K/(e^K - e^{-K})$  that is calculated by MCNP. In this example we specify  $p(\mu) = Ce^{2\mu}$  so that 50% of all source particles are emitted within 48 degrees of the x-axis. Here the forward-to-backward emission probabilities,  $p(1)/p(-1) = e^{-4} \simeq 1/54.5$ .

Another approach for source direction biasing is to restrict source emission to a set of nested cones about the bias direction. This discontinuous conical biasing is more time consuming to implement but can produce better results, when optimized, than can the continuous direction biasing. In some problems involving a collimated source, it must be used. Suppose we set up a set of nested cones about the source parameter VEC direction with cosines of the conical half angles  $-1 < \mu_1 < \mu_2 < \dots < \mu_n < 1$ . We want particles to be emitted in  $\mu_{i-1} < \mu < \mu_i$  with probability  $p_i$  (here  $\mu_0 \equiv -1$

and  $\mu_{n+1} \equiv 1$ ). Then on the SDEF card place the parameter DIR = dn with the following lines placed after the SDEF card:

```

SIn  -1   $\mu_1$   $\mu_2$  ...  $\mu_n$  1
SPn   0   $f_1$   $f_2$  ...  $f_n$   $f_{n+1}$ 
SBn   0   $p_1$   $p_2$  ...  $p_n$   $p_{n+1}$ 

```

Here  $f_i$  is the fraction of the solid angle of the i-th cone and is calculated as  $f_i = [\mu_i - \mu_{i-1}]/2$ .

## 4.5 Final Recommendations

Here are some recommendations for using the various variance reduction techniques.

- Before attempting to use variance reduction techniques for the first time, use the contemplated technique on a simple problem before using it on the practical and more complex problem. You need to get a feel for how the technique works without the confounding complexities of a difficult problem.
- One of the key parameters for assessing the effectiveness of different variance reduction techniques for your problem is the figure-of-merit (FOM). Generally, the better the improvement in the FOM, the better is the variance reduction technique.
- For deep penetration problems, use either cell importances or (preferably) weight windows to keep the particle population high in the cells of interest. Weight windows is more difficult to implement but more effective when done correctly. However, geometry splitting through cell importances is relatively safe and easier to implement.
- Use the CUT, ELPT, and PHYS commands when appropriate to avoid time-consuming tracking, physic, or unimportant tally contributions. This can speed up calculational times for some problem by a factor of 10.

## 5 MCNP Output

The output produced by MCNP provides a wealth of information about the simulation. The skill of the analyst is in using this output to interpret the precision and acceptability of the tally results produced by the Monte Carlo run and to decide what changes need to be made to improve the tally in subsequent runs.

### 5.1 Output Tables

§5.13.3

MCNP provides a wealth of information about the simulation, and a skilled user can elicit much insight from this voluminous output. By default only a small portion of all the possible output is produced. Always output are (1) input file listing, (2) summary of particle loss/creation, (3) summary of KCODE cycles (if KCODE is used), (4) tallies (if used), and (5) tally fluctuations charts. In addition, certain output tables deemed *basic* are always produced—they cannot be avoided. Other *default* tables are also generated unless turned off by the PRINT command. The various MCNP tables are listed in Table 7.

The output is changed from the default with the PRINT command in Block 3 of the input. Examples of the three forms of this command are

```

PRINT                $ produce everything
PRINT  110  20       $ basic & default tables plus Tables 110 and 20
PRINT -110 -20       $ all Tables except Tables 110 and 20

```

**Table 7.** Selected output tables available in MCNP. (*d*)=*default*; (*b*)=*basic*

Table No.	Table Description	Table No.	Table Description
10	Source information	120	Importance function analysis
20	Weight windows information	126	Cell particle activity
30	Tally descriptions	128( <i>b</i> )	Universe map
35	Coincident detectors	130	Particle weight balances
40	Material compositions	140	Neutron/photon nuclide activity
50	Cell vols & masses; surface areas	150	DXTRAN diagnostics
60( <i>b</i> )	Cell importances	160( <i>d</i> )	TFC bin tally analysis
62( <i>b</i> )	Forced coll.; expon. transform	161( <i>d</i> )	$p(x)$ tally PDF plot
70	Surface coefficients	162( <i>d</i> )	Cumulative $p(x)$ plot
72( <i>b</i> )	Cell temperatures	170	Source frequency; surface source
85	Electron range & straggling	175	Estimated $k_{eff}$ by cycle
90	KCODE source data	178	Estimated $k_{eff}$ by batch size
98	Physics const.& compile options	180	WWG bookkeeping summary
100( <i>b</i> )	Cross section tables	190( <i>b</i> )	WWG summary
102	S( $\alpha, \beta$ ) nuclide assignment	198	WW from multigroup fluxes
110	First 50 starting histories	200( <i>b</i> )	WW generated windows

## 5.2 Accuracy versus Precision

§2.6.2

With MCNP and its various variance reduction techniques, it is possible (and often the case for novice users) to produce tally results that, while very *precise*, i.e., a small relative error, are not very *accurate*. Technically, *precision* is the uncertainty (as measured by the tally variance) in the tally mean  $\bar{x}$  caused by the statistical fluctuations in the individual scores  $x_i$  of the simulated histories. By contrast, *accuracy* is a measure of how close the tally mean  $\bar{x}$  is to the true physical quantity being estimated. The difference between the true value and the expectation value of the simulation tally is called the *systematic error*, an important quantity but one that is seldom known.

### Factors Affecting Accuracy:

§2.6.2.1

- *The MCNP code:* This includes inaccuracies introduced by MCNP in its use of (1) physics models, (2) mathematical models, (3) uncertainties in the nuclear/atomic data, including cross sections, atomic weights, Avogadro’s number, etc., and (4) coding errors. MCNP is a very mature code and these sources of error, while always present, are not generally thought to be a major concern for “standard neutron/photon problems.” Many MCNP benchmark validation problems have been analyzed and documented.
- *The MCNP model:* Improper modeling of source energy and angular distributions, poor representation of the actual geometry by the MCNP geometric model, and errors in the material compositions can lead to significant inaccuracies.
- *User errors:* Probably the most important source of inaccuracies (at least for novices) is error introduced by the user in incorrectly using program options or making errors in the input file. Similarly, a novice often misunderstands the difference between a particular tally and the physical quantity being sought.

### Factors Affecting Precision:

§2.6.2.2

- *Forward versus adjoint calculations:* For problems with spatially extended sources and a tally in a small region, an adjoint simulation often produces more precise results with few histories compared to a forward simulation.

- *Tally type*: The choice of tally type often greatly affects the precision of the results. For example, point detectors are often less precise than surface detectors in a scattering medium.
- *Variance reduction*: The use of different variance reduction techniques can affect the tally precision tremendously.
- *Number of histories*: The more histories run (and the greater computer effort expended) the better will be the precision of the tallies.

### 5.3 Statistics Produced by MCNP

MCNP produces a wealth of information about a simulation to allow the user to assess the *precision* (not the accuracy) of the result. While much of the detailed assessment performed by an experienced user depends on careful examination of the many output tables, the initial focus should be on the ten statistical indices calculated by MCNP. In this section we review these ten statistics.

#### 5.3.1 Relative Error

§2.6.4

Many beginners examine only the relative error  $R$ , and, while this is a very important statistic, it alone cannot decide the acceptability of the tally result. The relative error is the fractional 1-sigma estimated uncertainty in the tally mean, i.e.,  $R \equiv S_{\bar{x}}/\bar{x}$ , the ratio of the standard deviation of the tally mean to the mean. Here is how  $R$  is to be used to interpret the tally value:

**Table 8.** Interpretation of the relative error  $R$ .

Range of $R$	Quality of Tally
$> 0.5$	Meaningless
0.2 to 0.5	Factor of a few
$< 0.1$	Reliable (except for point/ring detectors)
$< 0.05$	Reliable even for point/ring detectors

The value of  $R$  is determined by two quantities: (1) the history scoring efficiency  $q$ , which is the fraction of histories producing non-zero  $x_i$ 's, and (2) the dispersion in nonzero scores. In almost every tally, the tally PDF  $f(x)$  (whose mean the tally is trying to estimate) has a delta-function at  $x = 0$  representing the probability a source particle makes no contribution to the tally (e.g., a source particle is absorbed before reaching the tally region).

MCNP breaks  $R$  up into two components such that  $R^2 = R_{eff}^2 + R_{imp}^2$ . Here  $R_{eff}$  is the spread in  $R$  caused by scoring inefficiency and  $R_{imp}$  is the intrinsic spread of the non-zero history-scoring events. If every source particle contributes to the tally ( $q = 1$ ) then  $R_{eff} = 0$ ; but as more and more particles produce zero score,  $R_{eff}$  increases. By contrast,  $R_{imp}$  measures the uncertainty produced by the spread of nonzero scoring events. If some particles produce zero scores and the remainder produce the *same score*,  $R_{imp} = 0$ . As the scoring particles have increasingly different scores,  $R_{imp}$  increases.

The purpose of variance reduction techniques is to increase the scoring efficiency  $q$  and hence to reduce  $R_{eff}$ . At the same time we want to decrease the spread in nonzero scores, i.e. to make  $f(x)$  more concentrated about its mean so that  $R_{imp}$  decreases.

#### 5.3.2 Figure of Merit

§2.6.5

Another important statistic generated by MCNP is the *figure of merit* (FOM), defined as

$$\text{FOM} = \frac{1}{R^2 T}, \quad (10)$$

where  $T$  is the run time. Since  $T$  varies with the computer, the same simulation performed on different machines produces different FOMs. As discussed earlier in Section 4.1.1, the FOM should remain relatively constant (except for fluctuations early in the simulation). For different variance reduction techniques, the one with the largest FOM is preferred.

### 5.3.3 Variance of the Variance

The estimation of the relative error  $R$  is important to indicate the precision of the tally mean. However, how accurate is the estimation of  $R$ ? To indicate the accuracy of  $R$ , MCNP estimates the relative variance of  $R$ , i.e. a variance of a variance (VOV). The VOV is defined as

§2.6.7

$$\text{VOV} = \frac{S^2(S_{\bar{x}}^2)}{S_{\bar{x}}^2} = \frac{\sum_{i=1}^N (x_i - \bar{x})^4}{\left[\sum_{i=1}^N (x_i - \bar{x})^2\right]^2} - \frac{1}{N}. \quad (11)$$

where  $S^2(S_{\bar{x}}^2)$  is the variance of  $S_{\bar{x}}^2$ .

The VOV involves the third and fourth moments of the tally distribution  $f(x)$  and is much more sensitive to fluctuations in large history scores than is  $R$ , which is based on only the first and second moments of  $f(x)$ . The proper sampling of infrequent but high scoring events is vital if reliable tally means are to be obtained, and for this reason the VOV is an important indicator of a reliable result.

From Eq. (11), it can be shown that the VOV should decrease as  $1/N$ . MCNP tests for this  $1/N$  behavior in the VOV. Further, the VOV should always be less than 0.1 for all types of tallies.

### 5.3.4 The Empirical PDF for the Tally

MCNP also constructs the tally PDF  $f(x)$  to help assess the quality of the confidence interval estimates for the tally mean. An example is shown in Fig. 11. Examination of the high-end tail of this distribution is very important for problems involving infrequent events with very high score. Three possible outcomes for such problems are possible:

§2.6.8

1. Statistically meaningful confidence intervals are produced. This, of course, is always the desired outcome.
2. The sampling of a rare event with a very large score causes the the mean and  $R$  to increase and the FOM to decrease significantly. This situation is easily detected by observing the behavior of  $R$  and FOM in the tally fluctuation chart (TFC) produced at the end of the MCNP output. See Fig. 12 for a well-behaved example.
3. The third and most troublesome case is one that appears to be converged, based on acceptable statistical behavior of the mean,  $R$ , FOM, and the VOV, but in reality the tally mean is substantially underestimated because large scoring histories were inadequately sampled. Detecting this situation of too few large history tallies is difficult. It is for this case that MCNP performs extensive analysis of the high tally tail of the tally PDF.

The main difficulty in detecting case 3 above is knowing when you have performed enough histories to make a valid estimate of the confidence interval for the tally mean. The *central limit theorem* (CLT) guarantees the tally mean will appear to be sampled from a normal distribution with a standard deviation  $\sigma/N$  if  $N$  is sufficiently large. The confidence intervals estimated by MCNP for the tally are based on this normality assumption. The key question is how large must  $N$  be for this assumption to be valid.

For the CLT to hold, the first two moments of the tally PDF  $f(x)$ ,  $E(x) = \int_0^\infty x f(x) dx$  and  $E(x^2) = \int_0^\infty x^2 f(x) dx$ , must exist.<sup>12</sup> For the first two moments to exist,  $f(x)$  must either have a

<sup>12</sup>For the VOV to be finite, the third and fourth moments must also exist; however, MCNP doesn't enforce this.

fom = (histories/minute)\*(f(x) signal-to-noise ratio)\*\*2 = (4.861E+03)\*( 5.450E-02)\*\*2 = (4.861E+03)\*(2.971E-03) = 1.444E+01  
 unnormed tally density for tally 14 nonzero tally mean(m) = 3.961E-12 nps = 200000 print table 161

abscissa	ordinate	log plot of tally probability density function in tally fluctuation chart bin(d=decade,slope= 3.9)			
tally number	num den	log den	d	d	d
3.16-16	1 7.69+10	10.886	*****	*****	*****
3.98-16	0 0.00+00	0.000			
5.01-16	0 0.00+00	0.000			
6.31-16	0 0.00+00	0.000			
7.94-16	0 0.00+00	0.000			
1.00-15	0 0.00+00	0.000			
1.26-15	0 0.00+00	0.000			
1.58-15	0 0.00+00	0.000			
2.00-15	0 0.00+00	0.000			
2.51-15	0 0.00+00	0.000			
3.16-15	0 0.00+00	0.000			
3.98-15	0 0.00+00	0.000			
5.01-15	0 0.00+00	0.000			
6.31-15	0 0.00+00	0.000			
7.94-15	0 0.00+00	0.000			
1.00-14	1 2.43+09	9.386	*****	*****	*****
1.26-14	0 0.00+00	0.000			
1.58-14	5 7.67+09	9.885	*****	*****	*****
2.00-14	3 3.66+09	9.563	*****	*****	*****
2.51-14	2 1.94+09	9.287	*****	*****	*****
3.16-14	3 2.31+09	9.363	*****	*****	*****
3.98-14	5 3.05+09	9.485	*****	*****	*****
5.01-14	9 4.37+09	9.640	*****	*****	*****
6.31-14	8 3.08+09	9.489	*****	*****	*****
7.94-14	9 2.75+09	9.440	*****	*****	*****
1.00-13	8 1.94+09	9.289	*****	*****	*****
1.26-13	10 1.93+09	9.286	*****	*****	*****
1.58-13	15 2.30+09	9.362	*****	*****	*****
2.00-13	20 2.44+09	9.387	*****	*****	*****
2.51-13	27 2.61+09	9.417	*****	*****	*****
3.16-13	23 1.77+09	9.248	*****	*****	*****
3.98-13	45 2.75+09	9.439	*****	*****	*****
5.01-13	57 2.76+09	9.442	*****	*****	*****
6.31-13	83 3.20+09	9.505	*****	*****	*****
7.94-13	69 2.11+09	9.325	*****	*****	*****
1.00-12	62 1.51+09	9.178	*****	*****	*****
1.26-12	71 1.37+09	9.137	*****	*****	*****
1.58-12	90 1.38+09	9.140	*****	*****	*****
2.00-12	72 8.77+08	8.943	*****	*****	*****
2.51-12	76 7.36+08	8.867	*****	*****	*****
3.16-12	74 5.69+08	8.755	*****	*****	*****
3.98-12	84 5.13+08	8.710	mmmmmmmmmmmmmmmmmmmm	mmmmmmmmmmmmmmmmmmmm	mmmmmmmmmmmmmmmmmmmm
5.01-12	70 3.40+08	8.531	*****	*****	*****
6.31-12	89 3.43+08	8.535	*****	*****	*****
7.94-12	68 2.08+08	8.318	*****	*****	*****
1.00-11	78 1.90+08	8.278	*****	*****	*****
1.26-11	77 1.49+08	8.172	*****	*****	*****
1.58-11	60 9.20+07	7.964	*****	*****	s
2.00-11	18 2.19+07	7.341	*****	s	
2.51-11	8 7.74+06	6.889	*****	s	
3.16-11	1 7.69+05	5.886	*	s	
3.98-11	3 1.83+06	6.263	*****	s	
total	1404 7.02-03		d-----d	d-----d	d-----d

Figure 11. An example of the Tally PDF plot produced in the MCNP output.

---

nps	tally 4				fom	tally 14				fom
	mean	error	vov	slope		mean	error	vov	slope	
16000	2.5565E-19	0.1546	0.0460	0.0	13	1.6147E-20	0.1550	0.0990	0.0	13
32000	2.6267E-19	0.1057	0.0219	0.0	14	1.5614E-20	0.1098	0.0404	0.0	13
48000	2.9321E-19	0.0822	0.0129	10.0	15	1.5964E-20	0.0868	0.0228	0.0	13
64000	2.9096E-19	0.0725	0.0108	10.0	14	1.6062E-20	0.0760	0.0189	0.0	13
80000	2.9088E-19	0.0655	0.0086	10.0	14	1.6037E-20	0.0687	0.0161	4.9	13
96000	2.9487E-19	0.0595	0.0072	10.0	14	1.5578E-20	0.0631	0.0130	2.7	13
112000	2.9758E-19	0.0545	0.0061	10.0	15	1.5749E-20	0.0571	0.0105	3.0	13
128000	3.0167E-19	0.0509	0.0052	10.0	15	1.5970E-20	0.0528	0.0086	2.7	14
144000	3.0142E-19	0.0483	0.0050	10.0	14	1.5824E-20	0.0496	0.0075	2.7	14
160000	3.0284E-19	0.0461	0.0046	10.0	14	1.6205E-20	0.0465	0.0064	2.8	14
176000	3.0391E-19	0.0443	0.0042	10.0	14	1.6276E-20	0.0441	0.0056	3.2	14
192000	3.0143E-19	0.0427	0.0040	10.0	14	1.6351E-20	0.0420	0.0050	3.5	14
200000	3.0080E-19	0.0420	0.0040	10.0	14	1.6317E-20	0.0410	0.0048	3.9	14

---

**Figure 12.** Example of a tally fluctuation chart (TFC).

finite upper tally cutoff, or decrease with  $x$  faster than  $1/x^3$ . It is this behavior of a proper tally PDF that MCNP tests for by analyzing the high-tally tail of the empirical PDF.

MCNP uses the highest scoring histories (the 200 largest) to estimate the slope of the PDF's high-tally tail. This is done by fitting a generalized Pareto function (with parameters  $a$  and  $k$ ), namely

$$f_{\text{Pareto}}(x) = \frac{1}{a(1 + kx/a)^{1+(1/k)}}, \quad (12)$$

to the high tally events. The slope is then estimated from

$$\text{SLOPE} = 1 + \frac{1}{k} \quad (13)$$

On the output plot of the PDF, the Pareto fit is shown by string of s's, and tally mean by a row of m's (see Fig. 7).

For the high-end tail to be acceptable, a sufficient number of histories has to have been run so that the CLT is expected to apply, namely, the SLOPE must be 3 (or greater). If insufficient, rare, high-scoring events have not been tallied, the SLOPE will generally not satisfy this criterion. If too few histories have been run to estimate the slope, the SLOPE is reported as 0; if the PDF falls off faster than  $1/x^{10}$ , the SLOPE is set to 10 (a "perfect" value).

### 5.3.5 Confidence Intervals

From the relative error  $R$ , MCNP estimates the confidence interval for the tally. Because the estimated mean and estimated uncertainty in the mean are correlated, the mid-point of the confidence interval needs to be shifted slightly from the mean. The amount of this midpoint shift, SHIFT, is proportional to the third central moment, and should decrease as  $1/N$ . MCNP calculates this refinement for the confidence interval.

§2.6.9

### 5.3.6 A Conservative Tally Estimate

Sometimes a user wishes to make a conservative tally estimate, just in case rare high-tally events may not be completely considered. In the output, MCNP shows what would happen to the mean,  $R$ , VOV, confidence interval, etc., if the next history ( $N + 1$ ) were the same as the largest scoring history encountered in the simulation of  $N$  histories. If large changes occur, then be very suspicious of the result.

§2.6.9.2.2

### 5.3.7 The Ten Statistical Tests

§2.6.9.2.3

The most valuable tool provided by MCNP for assessing the reliability of results is the suite of 10 statistical tests it performs on the tally. If any of the 10 tests are failed, MCNP automatically produces additional output to aid the user in interpreting the seriousness of the failed test(s). The 10 tests are summarized below.

#### Tally Mean, $\bar{x}$ :

1. The mean must exhibit, for the last half of the problem, only random fluctuations as  $N$  increases. No up or down trends must be exhibited.

#### Relative Error, $R$ :

2.  $R$  must be less than 0.1 (0.05 for point/ring detectors).
3.  $R$  must decrease monotonically with  $N$  for the last half of the problem.
4.  $R$  must decrease as  $1/\sqrt{N}$  for the last half of the problem.

#### Variance of the Variance, VOV:

5. The magnitude of the VOV must be less than 0.1 for all types of tallies.
6. VOV must decrease monotonically for the last half of the problem.
7. VOV must decrease as  $1/N$  for the last half of the problem.

#### Figure of Merit, FOM:

8. FOM must remain statistically constant for the last half of the problem.
9. FOM must exhibit no monotonic up or down trends in the last half of the problem.

#### Tally PDF, $f(x)$ :

10. The SLOPE determined from the 201 largest scoring events must be greater than 3.

If any of these tests fails, a warning is printed in the output and a plot of  $f(x)$  is produced. If all ten tests are passed, MCNP then calculates asymmetric and symmetric confidence intervals for the mean at the one-, two-, and three-sigma levels. While these ten statistical tests provided an excellent indication of the reliability of the result, *they are not foolproof*. There is always the possibility that some high-scoring rare event was not sampled in the histories run and that the tally is underestimated. Users must rely on their understanding and insight into the particular problem to avoid such traps.

### 5.3.8 Another Example Problem

Consider a point isotropic source of 7-MeV photons in an infinite medium of iron. The ambient dose equivalent 30 cm from the source is sought. A surface F2 detector and a F5 point detector are both used to estimate this dose. The input file is shown in Fig. 13.

The variation of the tally mean,  $R$ , VOV, SLOPE, and FOM with the number of particle histories is shown in Fig. 14. At  $10^7$  particle histories, the F2 tally passed all 10 statistical tests: the mean and FOM are relatively constant, the relative error  $R$  is monotonically decreasing as  $1/\sqrt{N}$  (1 y-decade decrease for every 2 x-decades increase), the VOV is monotonically decreasing as  $1/N$  (1 y-decade decrease for every 1 x-decade increase), and the SLOPE has a “perfect” value of 10. This high slope value is to be expected since there physically is an upper limit to the tally, namely that produced by an uncollided photon reaching the scoring surface. The slope of 10 is a strong indicator of such a tally cutoff.

By contrast, the F5 point detector has not converged. The mean, error, VOV, and FOM all exhibit sudden changes, a result of an occasional photon that scatters very near the point detector



and contributes a huge score with the last-flight estimator used by the F5 tally. The SLOPE remains constant at about 2, an indication of a long slowly decreasing high-tally tail. In fact, a point detector in a scattering medium has no tally cutoff. Be very wary of using point/ring detectors in a strongly scattering medium.

If you had performed this simulation for only 5000 histories and, unwisely, looked only at the relative errors, the F5 detector would appear attractive since it has a relative error of about 0.06 (almost near the acceptable value) while the F2 tally has  $R > .2$ . Recall that every source particle produces a score with a point detector ( $q = 1$ ,  $R_{eff} = 0$ ) and  $R$  often starts to decrease properly. The F2 tally, on the other hand, received scores from only 0.8% ( $q = 0.0080$ ) of the source particles leading to  $R_{eff} = 0.0024$  and  $R_{imp} = 0.0024$  after  $10^7$  histories. Because of the large fluctuations in the F5 scores, its  $R_{imp}$  is much larger (0.127 after  $10^7$  histories).

The PDFs for these two tallies are shown in Figs. 15 and 16. As expected, the PDF for the F5 tally is spread out over a wide range of scores and has a high-score tail that is poorly defined even after  $10^7$  histories. The PDF for the F2 tally is much more compact with a well established upper cutoff.

---

```

Point isotropic 7-MeV photon sources in infinite iron medium
c ***** BLOCK 1: CELL CARDS *****
  1 1  -7.86  -10      imp:p=1  $ iron inside detector shell
  2 1  -7.86  10 -20    imp:p=1  $ iron outside detector shell
  3 0           20      imp:p=0  $ vacuum outside problem boundary

c ***** BLOCK 2: SURFACE CARDS *****
  10 so 30.0          $ detector surface
  20 so 3000.0       $ outer surface of iron

c ***** BLOCK 3: DATA CARDS *****
SDEF  erg=7.00  par=2      $ pt isotropic 7-MeV photon source
mode  p                    $ photon mode only
nps   1000000             $ number of histories to be run
f2:p  10                  $ tally 2:  surface detector at 30 cm
f15:p 30 0 0 -0.3        $ tally 15: pt det 30 cm on x-axis; Ro=.3mfp
c
c --- Photon ambient dose equivalent H*(10mm) Sv cm^2; from ICRP [1987]
de    0.100E-01 0.150E-01 0.200E-01 0.300E-01 0.400E-01 0.500E-01
      0.600E-01 0.800E-01 0.100E+00 0.150E+00 0.200E+00 0.300E+00
      0.400E+00 0.500E+00 0.600E+00 0.800E+00 0.100E+01 0.150E+01
      0.200E+01 0.300E+01 0.400E+01 0.500E+01 0.600E+01 0.800E+01 0.100E+02
df    0.769E-13 0.846E-12 0.101E-11 0.785E-12 0.614E-12 0.526E-12
      0.504E-12 0.532E-12 0.611E-12 0.890E-12 0.118E-11 0.181E-11
      0.238E-11 0.289E-11 0.338E-11 0.429E-11 0.511E-11 0.692E-11
      0.848E-11 0.111E-10 0.133E-10 0.154E-10 0.174E-10 0.212E-10 0.252E-10
c
m1    26000  -1.00000      $ natural iron (density 7.86 g/cm^3)

```

---

**Figure 13.** Input file for the example problem

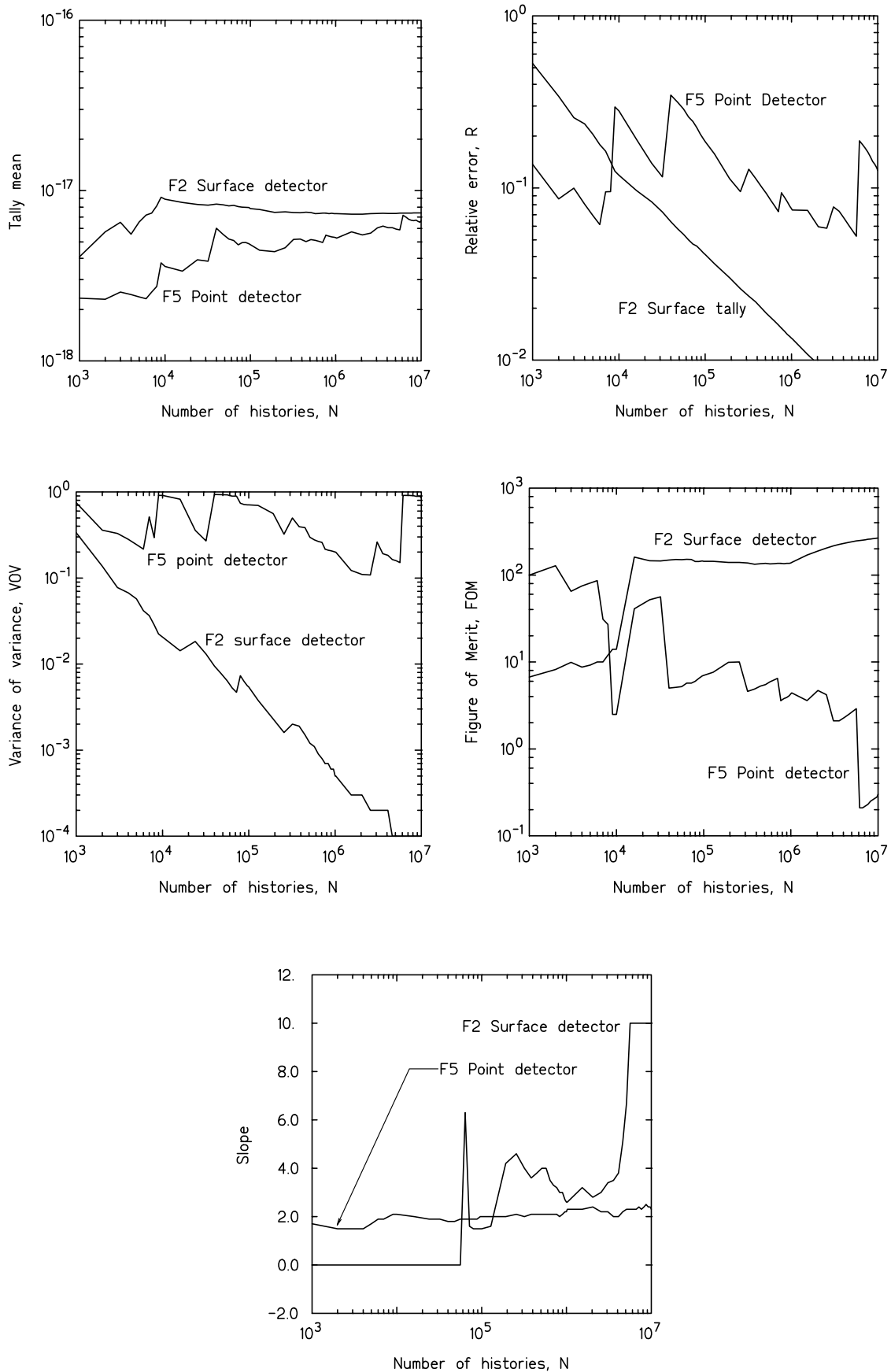


**Figure 14.** The variation of the various statistics estimated by MCNP for the two tallies of the test problem of Fig. 13.

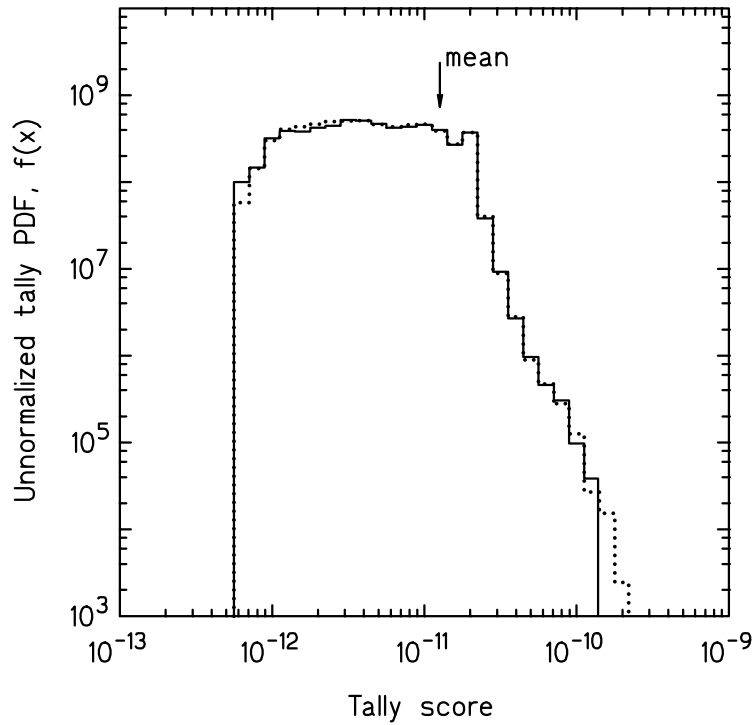


**Figure 15.** The PDF for the F2 surface tally in the example problem. Heavy line is for  $10^6$  histories and dotted line for  $10^7$ .

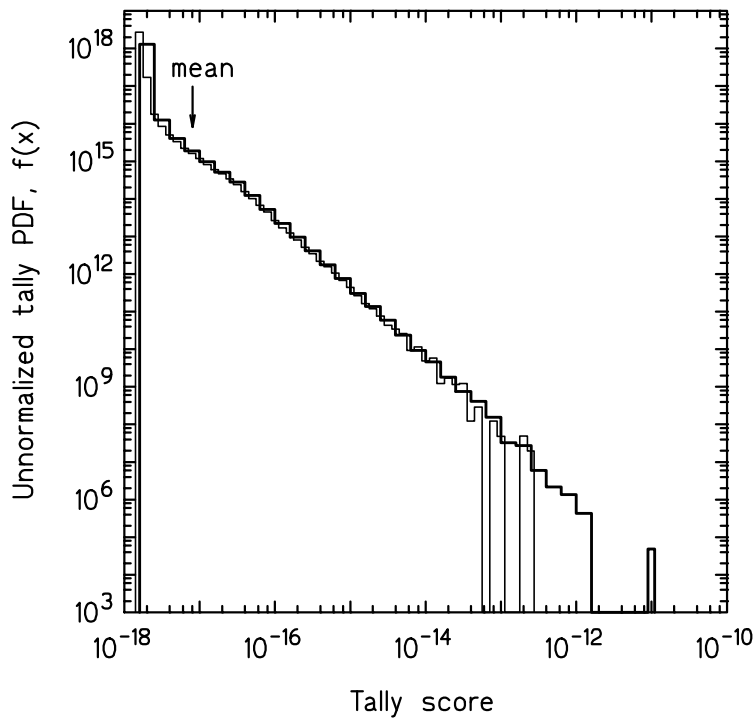


**Figure 16.** The PDF for the F5 tally in the example problem. Light line is for  $10^6$  histories and the heavy line for  $10^7$ .

## Useful Web Sites

[https://mcnp.lanl.gov/reference\\_collection.html](https://mcnp.lanl.gov/reference_collection.html). This is the official web site for MCNP. Much MCNP information is available from this site including the *Theory & User's Manual* and a large number number of Los Alamos Technical Reports presenting many different details about the code.

<https://nucleardata.lanl.gov/>: This site provides the latest cross section and related data in the ASCII ACE format needed by MCNP. As errors in the ENDF/B files are corrected or updated, new ACE formatted files are found here.

<https://www.nndc.bnl.gov/>. This is the official site for the national nuclear data center from which a wealth of nuclear data can be obtained. In particular, the latest ENDF/B cross sections are readily available in ASCII or graphical form.

## REFERENCES

CONLIN J.L. (Ed.) AND the LANL Nuclear Data Team, XCP-5, *Listing of Available ACE Data Tables*, Technical Report LA-UR-17-20709, Oct. 2017, Los Alamos National Laboratory, Los Alamos, NM, USA. Available at [https://mcnp.lanl.gov/reference\\_collection.html](https://mcnp.lanl.gov/reference_collection.html).

DETWILER R.S., R.J. MCCONN, T.F. GRIMES, S.A. UPTON, AND E.J. ENGGEL, *Compendium of Material Composition Data for Radiation Transport Modeling*, Technical Report 200-DMAMC-128170 PNNL-15870, Rev. 2, April 2021, Pacific Northwest National Laboratory, Richland, WA, USA. Available at [https://www.pnnl.gov/main/publications/external/technical\\_reports/PNNL-15870Rev2.pdf](https://www.pnnl.gov/main/publications/external/technical_reports/PNNL-15870Rev2.pdf)

DUNN, W.L. AND J.K. SHULTIS, *Exploring Monte Carlo Methods*, 2ed, Academic Press, Elsevier, Cambridge, MA, USA, 2023.

KULESZA, Joel A. (Ed.) and 28 others, *MCNP<sup>®</sup> Code Version 6.3.0 Theory & User Manual*, Technical Report LA-UR-22-30006, Rev. 1, Sept. 28, 2022, Los Alamos National Laboratory, Los Alamos, NM, USA. Available at [https://mcnp.lanl.gov/reference\\_collection.html](https://mcnp.lanl.gov/reference_collection.html).

SHULTIS, J.K. AND R.E. FAW, *Radiation Shielding*, Amer. Nucl. Soc., LaGrange Park, IL, USA, 2000.